Analytical Modelling of Transverse Flux Motor Using Magnetic Equivalent Circuit and 3D FEM Analysis

By
Sheikh Ifatur Rahman (Student ID: 122427)
GNM Mushfiqur Mubin (Student ID: 122448)
Tajbir Hasan (Student ID: 122458)

A Thesis Submitted to the Academic Faculty in Partial Fulfillment of the Requirements for the Degree of
BACHELOR OF SCIENCE IN ELECTRICAL AND ELECTRONIC ENGINEERING

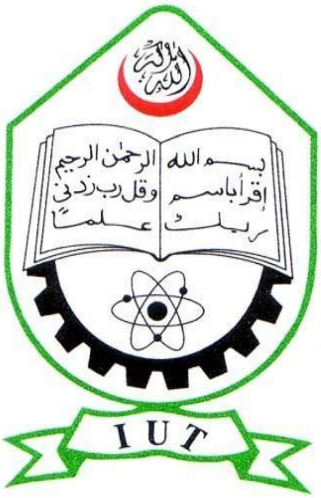

Department of Electrical and Electronic Engineering

Islamic University of Technology (IUT)
Gazipur, Bangladesh

November 2016

Declaration of Candidate

It is hereby declared that this thesis or any part of it has not been submitted elsewhere for the award of any Degree.

Approved by

_____

Prof. Dr. Md. Ashraful Hoque
Head of Department
Department of Electrical and Electronic Engineering,
Islamic University of Technology (IUT),
Boardbazar, Gazipur-1704.
Date:

Supervised by

_____

Prof. Dr. Kazi Khairul Islam
Department of Electrical and Electronic Engineering,
Islamic University of Technology (IUT),
Boardbazar, Gazipur-1704.
Date:

Iftekhar Hasan

_____

Iftekhar Hasan, Lecturer (on leave)
Department of Electrical and Electronic Engineering,
Islamic University of Technology (IUT),
Boardbazar, Gazipur-1704.
Date:

Submitted by

Sheikh Ifatur Rahman
Student ID: 122427
Academic Year: 2013-2016
Date:

GNM Mushfiqur Mubin
Student ID: 122448
Academic Year: 2013-2016
Date:

Tajbir Hasan
Student ID: 122458
Academic Year: 2013-2016
Date:

Table of Contents

List of Tables

List of Figures

Acknowledgements

We are grateful to our thesis supervisor, Prof. Dr. Kazi Khairul Islam sir, for his continuous guidance and motivation and ideas in out thesis topic.
We would also like to thank Iftekhar Hasan, lecturer of the department of Electrical and Electronic Engineering, Islamic University of Technology, for providing us with necessary information about Transverse Flux Motor and for his continuous help with the thesis. Without his constant demand for making the work more elaborate finally resulted in satisfactory and successful outcomes.

Abstract

This thesis presents the design one unique single phase transverse flux machines (TFM) with one rotor disk. The necessity to use three dimensional finite element analysis (FEA) justified by analyzing a U-core, which is a fundamental element of the magnetic circuit in the TFM. The analysis is performed under different conditions with different methods viz. MEC analytical method and 3D FEA. Analytical models for the modular TFM are derived in order to calculate the fluxes in the core created by magnets and the current in the stator winding, in terms of its geometrical parameters. The calculated fluxes are used to calculate the torque of the machine. The accuracy of the analytical models are evaluated by comparing the results with that obtained from 3D FEA for different loading conditions. The analytical models are then used to obtain some optimized geometrical configurations by assigning a range of to each geometrical parameter. By applying design constraints such as a low utilization of the magnetic cores and current densities than 5 A/mm2 in the conductors, some of the geometrical configurations can be eliminated.

Chapter 1- Introduction

1.1 Electrical Machines

Electric Machines are the most popular machines of everyday life and their number of types increases with developments in science, engineering and technology. Electric machines are used in a broad power range from mWs to 1.7GWs. To increase reliability and simplify maintenance of electromechanical drives, the dc commutator machine has gradually been replaced by an energy efficient cage induction motor and permanent magnet brushless motor.

In electrical engineering, electric machine is a general term for electric motors and electric generators. They are electromechanical energy converters: an electric motor converts electricity to mechanical power while an electric generator converts mechanical power to electricity. The moving parts in a machine can be rotating (rotating machines) or linear (linear machines). Besides motors and generators, a third category often included is transformers, which although they do not have any moving parts are also energy converters, changing the voltage level of an alternating current.

Electric machines, in the form of generators, produce virtually all electric power on Earth, and in the form of electric motors consume approximately 60% of all electric power produced. Electric machines were developed beginning in the mid19th century and since that time have been a ubiquitous component of the infrastructure. Developing more efficient electric machine technology is crucial to any global conservation, green energy, or alternative energy strategy.

1.2 Classifications

When classifying electric machines (motors and generators) it is reasonable to start with physical principle for converting electric energy to mechanical energy. If the controller is included as a part of the machine all machines can be powered by either alternating or direct current, although some machines will need a more advanced controller than others. Classification is complicated by the possibilities of combining physical principles when constructing an electrical machine.

1.2.1 DC Motors

A **DC motor** is any of a class of electrical machines that converts direct current electrical power into mechanical power. The most common types rely on the forces produced by magnetic fields. Nearly all types of DC motors have some internal

mechanism, either electromechanical or electronic, to periodically change the direction of current flow in part of the motor. Most types produce rotary motion; a linear motor directly produces force and motion in a straight line.

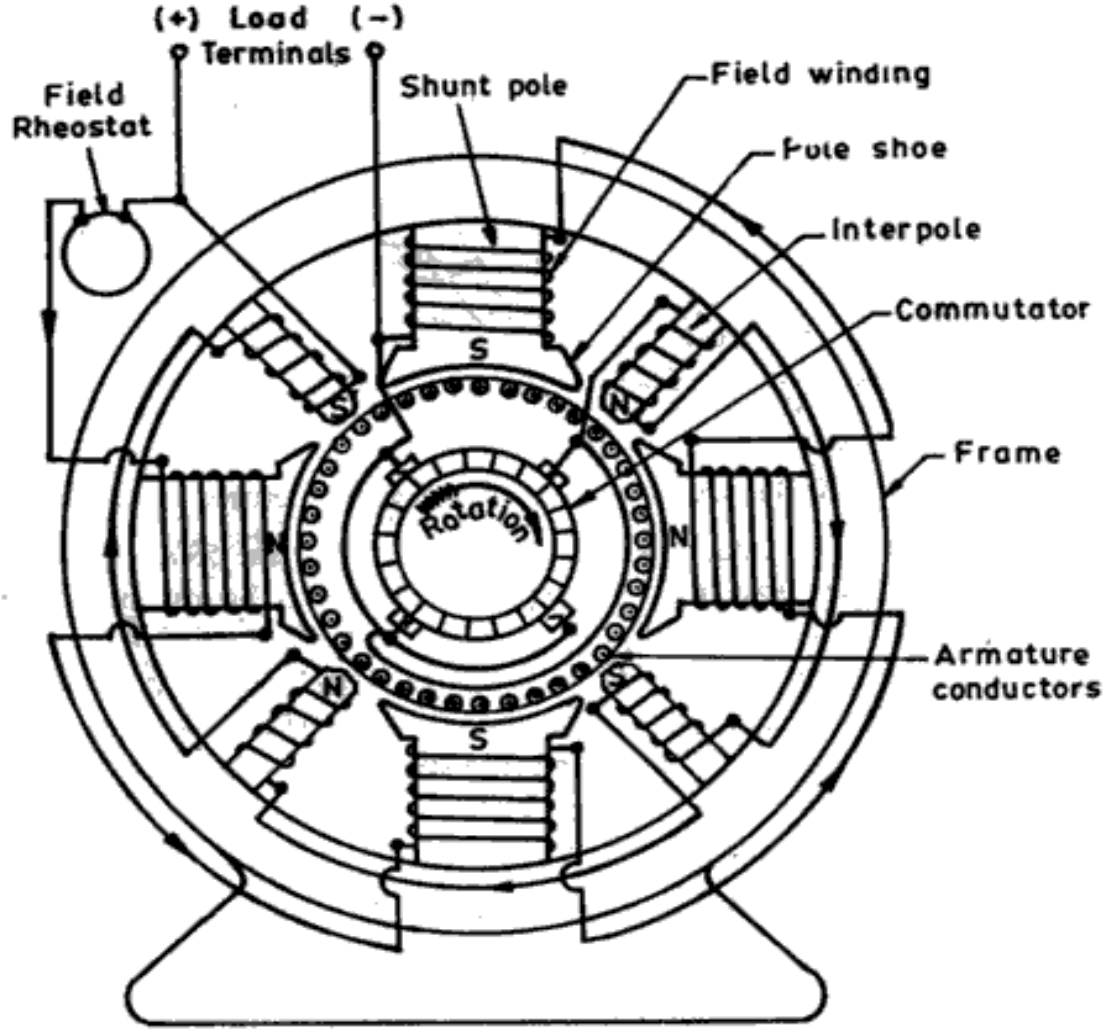

Figure 1.1: Construction of a typical DC motor

DC motors are of following types:

1. Shunt DC motor: The rotor and stator windings are connected in parallel.
2. Separately Excited motor: The rotor and stator are each connected from a different power supply, this gives another degree of freedom for controlling the motor over the shunt.
3. Series motor: the stator and rotor windings are connected in series. Thus the torque is proportional to I2 so it gives the highest torque per current ratio over all other dc motors. It is therefore used in starter motors of cars and elevator motors
4. Permanent Magnet (PMDC) motors: The stator is a permanent magnet, so the motor is smaller in size. It is only used for low torque applications.
5. Compounded motor: the stator is connected to the rotor through a compound

of shunt and series windings, if the shunt and series windings add up together, the motor is called commutatively compounded. If they subtract from each other, then a differentially compounded motor results, which is unsuitable for any application.

1.2.2 AC Motors

AC machines are motors that convert ac electric energy to mechanical energy and generators that convert mechanical energy to ac electric energy. The two major classes of ac machines are synchronous and induction machines. The field current of synchronous machines (motors and generators) is supplied by a separate dc power source while the field current of induction machines is supplied by magnetic induction (transformer action) into the field windings.

AC machines differ from dc machines by having their armature windings almost always located on the stator while their field windings are located on the rotor. A set of three-phase ac voltages is induced into the stator armature windings of an ac machine by the rotating magnetic field from the rotor field windings (generator action). Conversely, a set of three-phase currents flowing in the stator armature windings produces a rotating magnetic field within the stator. This magnetic field interacts with the rotor magnetic field to produce the torque in the machine (motor action).

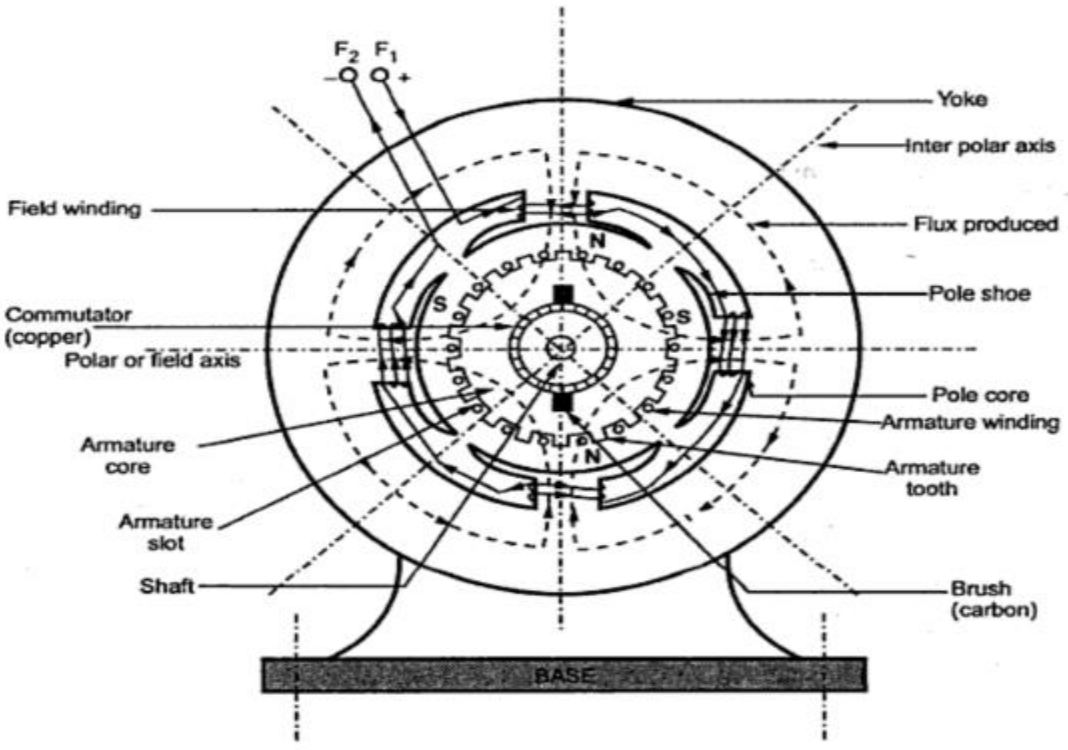

Figure1.2: Construction of AC Motor

• Induction Motor: Voltage is induced in the rotor (thus no need for brushes) of this type of motor, but for this to happen, the rotor must rotate at a lower speed than the magnetic field to allow for the existence of an induced voltage. Therefore, a new term is needed to describe the induction motor: the slip.
• Synchronous Motor: In this type of motor, the rotor tries to line up with the rotating magnetic field in the stator. It has the stator of an induction motor, and the rotor of a dc motor.

1.2.3 Other Special Motors

1. Reluctance motor: A synchronous-induction motor. The rotor has salient poles and a cage so that it starts like an induction motor. Brushless DC runs like a synchronous motor.
2. Hysteresis motor: Hysteresis produces the torque, can be very tiny, used as the driver for electric clocks.
3. Stepper motor: It is a special type of synchronous motors. It rotates a number of degrees with each electric pulse.
4. Brushless DC motor: A close cousin of a permanent magnet stepper motor with electronic controllers.
5. Universal motor: If a series dc motor has a laminated stator frame, it can run effectively from an ac supply as well as dc, this is the universal motor.

1.3 Contents of Thesis

Chapter 2 is comprised of the transverse lux motor concept where transverse flux concept has been discussed and a comparison of TFM is made with conventional motors.
Chapter 3 consists different types of TFM configurations with their figure.
Chapter 4 discusses the finite element method and also introduces the Maxwell 3D software along with some simulation done in the Maxwell software.
Chapter 5 discusses the Magnetic Equivalent Circuit Modelling with equations.
Chapter 6 discusses the results of the new transverse flux motor that has been designed analytically.
Chapter 7 concludes the whole thesis with future work possibilities.

Chapter 2- TFM Concept

2.1 Why Transverse Flux Motor?

During the recent past years, the to obtain more power from electrical machines with space and mass has increased rapidly. In other word the attention of engineers, researchers and scientists is drawn towards specific torque output, which is generally defined as torque per unit volume or unit mass. Electric vehicle propulsion ship propulsion and industrial robots are some of the applications which highly benefit from a high specific torque output.

Introduction of new permanent magnet material with increased remanence flux density has increased the specific outputs of electrical machines. However, since the stator teeth and the armature conductors compete for the same space, the magnet material cannot be fully utilized in conventional electrical machine designs.

The restriction on the conventional machines and the necessity to increase the specific output has led to the development of a new concept of machines called transverse flux topology.

2.2 Transverse Flux Concept

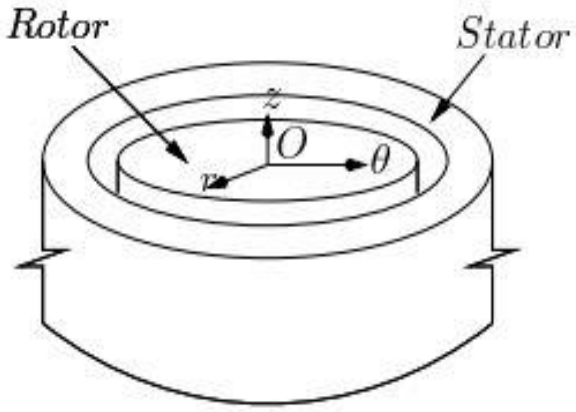

Figure 2.1: Simplified Representation of conventional machine.

In case of rotating machines, the flux lines have to be either radially or axially oriented in order- to be perpendicular to the direction of rotation. Then the direction of current in conductors has to be either- axially or radially oriented respectively to produce a force in the peripheral direction. The first case (Figure 2.1), with radial

flux and axial current, includes the synchronous and asynchronous or radial machines.

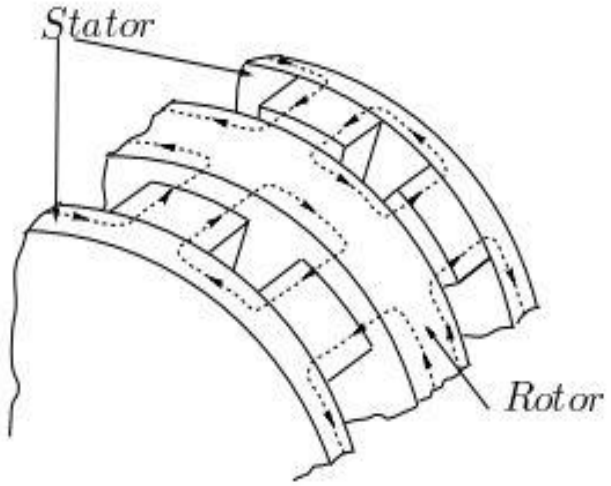

Figure 2.2: Simplified Representation of an axial flux machine

The second case with the excitation flux in the axial direction and current in the radial direction is shown in Figure 2.2. After the description of the magnetic and electrical circuits of the basic transverse flux machine topology, a check will be made to see whether the transverse flux machine obeys the same rules as the previously described machines.

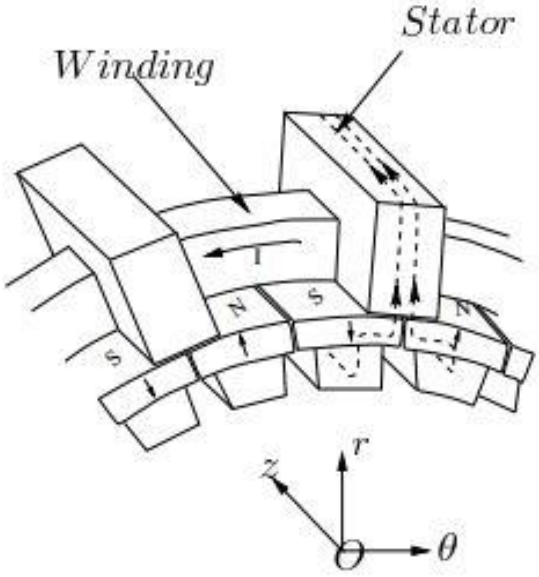

Figure 2.3: Basic Topology of Transverse flux machine

Figure 2.3 shows the basic topology of a transverse flux machine (TFM) and the 3D co-ordinate system as used in Figure 2.1. The dashed lines shown in the figure denote the path of the flux generated by the current in the winding. Permanent magnets

polarized radially are placed around the circumference of the rotor in an alternate manner. The second ring of permanent magnets axially displaced and ISO electrical degrees rotated relative to the first ring. are placed around the circular winding, one core per poll-pair (two magnets) of each ring. The path of the flux from the permanent magnets goes radially through the airgap into a leg of C-core, passing then axially along U-core, again radially inwards passing the airgap and magnet, and finally axially through the flux guiding elements under the magnets completing a plane which is parallel to rOz. The winding lies on the plane rog in the direction of motion. This type of the motor is called TFM due to the flux path being transversal to the speed vector.

2.3 Comparison of TFM with Conventional Machines

The specific output torque of any electrical machine can be either by increasing the air gap flux induction or by increasing the current loading of the armature. Increasing the airgap flux density requires to increase the teeth width to keep the level of saturation in the iron at a reasonable value. Increasing the current loading requires to increase the winding area to keep the level of the current density according to thermal capabilities. In brief, the strong competition for the same space by the stator teeth and the armature conductors sets restrictions to achieve high power- densities in the conventional machine arrangements.
In the basic topology shown in Figure 2.3, the advantage is that the stator teeth (C-cores) and the armature conductors are not competing for the same space any more. The conventional machines have the following features.

- The total mmf of the winding related to the electric loading, and is limited thermally.
- The maximum flux linkage seen by each turn of the winding is the per pole flux. This is inversely proportional to the number of poles and is limited by the magnetic loading.
- The spatial frequency of the magnetic flux directly proportional to the number of poles.

The transverse flux machines have the following characteristics.

- Larger coil cross sections can be achieved with a favorable slot design.
- Relatively small pole pitches are possible.
- The conductor length is relatively small and reduced to the circumferential dimension.
- The magnetically required may be dimensioned with restrictions and does not depend (so strongly) on the conductor cross-section.

- Since there is interaction between phases, fault in one phase does not bring the operation of the machine to standstill. There will be specific torque and more torque ripple in case of fault.
- In designs which achieve the highest specific torque, the magnet pole number tends to be high, producing a relatively high operating frequency, and core making the machines more suitable for low or moderate speeds.
- The flux-concentrating configurations are robust, which tends to limit operating speed.
- The power factor is generally low due to high leakage flux. Because of the high leakage flux that makes the flux path in third dimension as well, powdered soft magnet material are used to construct the stator of TFMs.

Chapter 3- TFM Configurations

Laithwaite et al mentioned that although the transverse flux concept was stated in 1904 and 1934 in German patents they were not developed further since no relative advantages were claimed. The publications by Prof. E.R. Laithwaite et al gave a new life to the machines with transverse flux for application in railway motored wheels. However, all these publications had focused on linear machines. Though the possibility of rotary machines with transverse flux concept was mentioned they were not discussed in detail due to their 'cumbersomeness'. Prof. H. Weh et al the rotary machines with transverse flux for the first time in detail — as far as it is known to the author.

3.1 Transverse Flux Configurations

Different machine configurations have been developed so far. However, the geometries are basically a one phase motor that can be transformed in a three phases motor without or with a very low magnetic coupling between the three phases. This feature simplifies the prediction of the performance of the machines as it can be deduced by analyzing single phase machine only.

3.1.1 Single Sided Transverse Flux Machines (SSTFM)

The simple arrangement of the SSTFM configuration shown in Figure 2.3. The armature winding is wound peripherally. The flux generated by the armature winding is conducted by the stator core pieces placed around the winding.

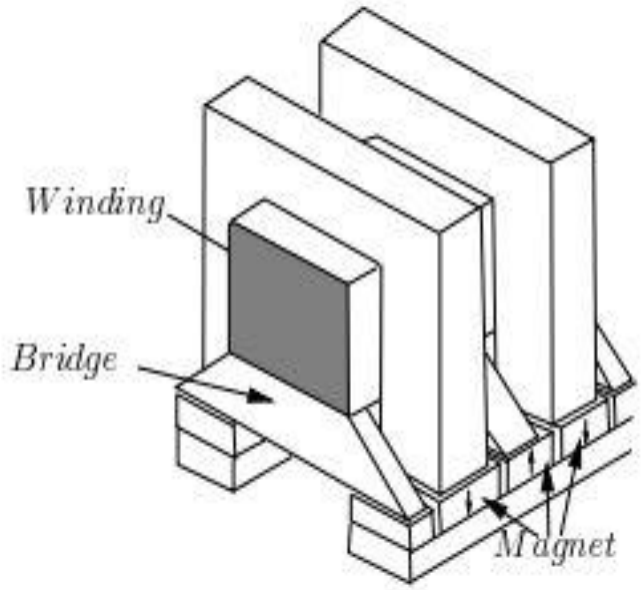

Figure 3.1 Single sided Transverse Flux Motor.

In case of the SSTFM, it is desirable to select an inner stator (outer rotor) concept due to following reasons:

- It is much wiser to wind the copper around the U cores than to fill into a slot in the inside of the cylinder.
- The ratio of airgap diameter to the outer diameter of the machine is greater because the rotor is thinner than the stator. This results in a large torque for the same volume of the motor.

The SSTFM is easier to construct than the other TFM arrangements.
There also another arrangement of the SSTFM which uses iron-bridge pieces and rotor magnets separated axially as shown in Figure 3.1.
This design has the advantage of eliminating unwanted iron material in the rotor. The bridges between the stator poles provide shunt paths for the magnet flux whose instantaneous linkage with the stator cores would otherwise be counter-productive for the torque. All the magnets are used at a given instant. However, there are some disadvantages of using the bridge topology. The available window for the stator winding is reduced due to the presence of bridges which also leads to the reduction of the stator excitation mmf. The bridges also attract significant leakage flux from the adjacent stator cores.

3.1.2 Double Sided TFM (DSTFM)

This configuration uses both sides of the rotor magnets. It has, in many ways, better performance than the SSTFM configuration. The arrangement of stator elements and rotor magnets is shown in Figure 3.2.

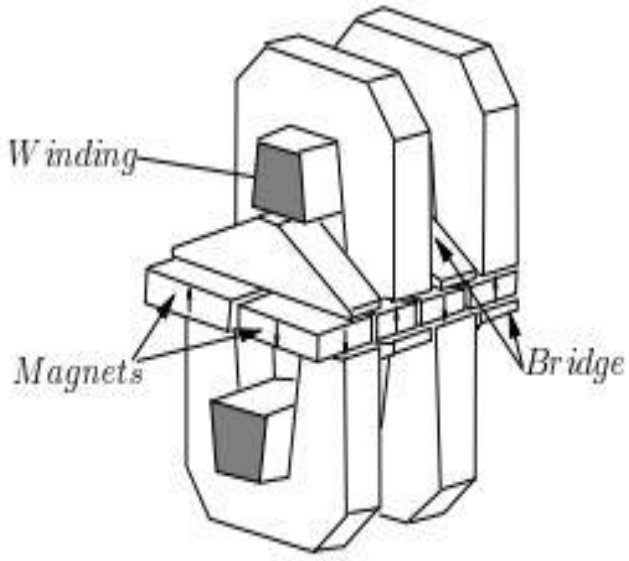

Figure 3.2: Double-sided TFM with bridge elements

The topologies of DSTFM have the active components of the rotor supported in a cantilevered arrangement, which seem-s both difficult to construct and tends to be mechanically weak unless measures are taken to strengthen the design.

3.1.3 Double-sided flux-concentrated TFM (DSFCTFM)

Here the rotor magnets are arranged in a flux concentrating geometry, which utilizes all of the magnetized magnets. The arrangement is illustrated in Figure 3.3.

This configuration also suffers from the following drawback:

The active components of the rotor are supported in a cantilevered arrangement, which seems both difficult to construct and can be mechanically weak except the variant shown in Figure which is mechanically stronger.

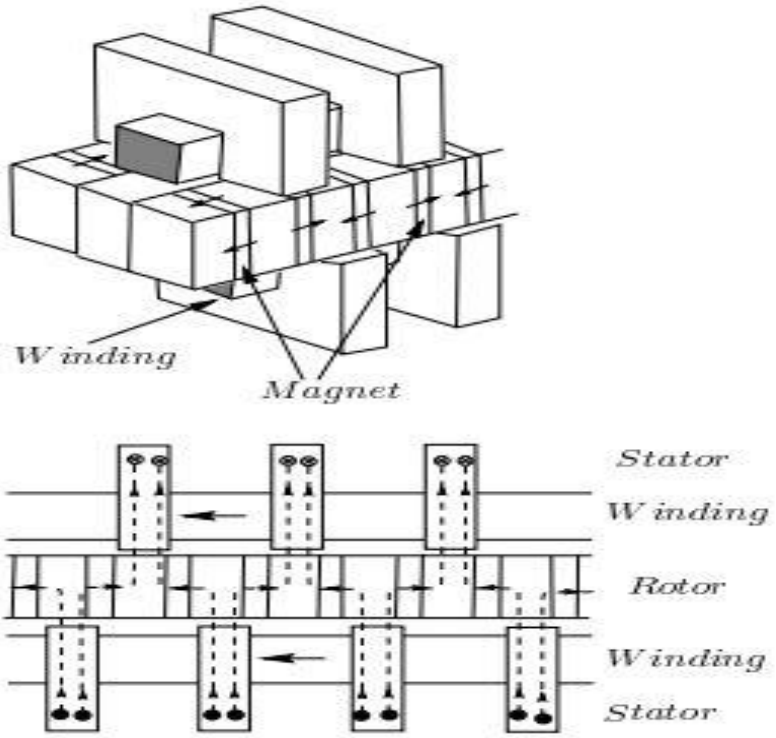

Figure 3.3: Double Sided flux concentrated TFM and its axial view with flux paths.

3.1.4 Claw-pole configuration

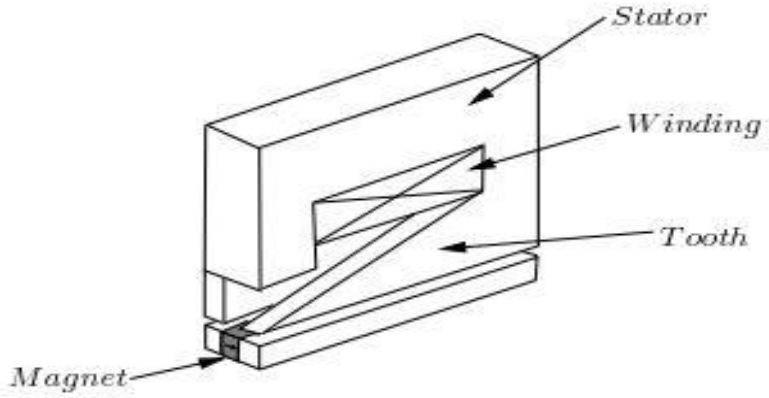

Figure 3.4: Claw-pole stator tooth

This configuration is basically the same as the SSTFM configuration. However, the shape of the stator cores, shown in Figure 3.4, differs from those of the SSTFM. The claw pole arrangement which uses the rotor magnets simultaneously has performances similar to the SSTFM. However, the overlapping tooth arrangement provides a short circuit path for approximately of the useful flux that enters the stator. This linkage flux limits the performance of the machine.

3.1.4 Z-TFM

In this configuration, the rotor magnets are magnetized in the radial directions similar to the SSTFM configuration, but the shapes of the stator teeth are different. Radial sectional views of the two peripherally adjacent stator cores are shown in Figure 3.5. This arrangement has the advantage of using all the magnets in the rotor unlike the SSTFM, which leads to a higher torque density and a better power factor.

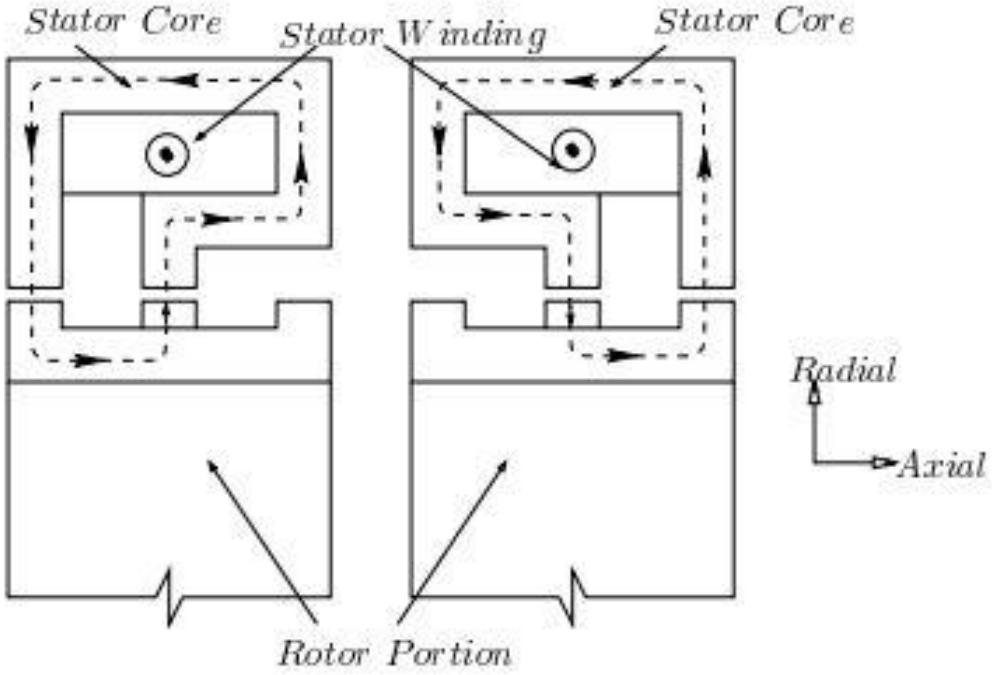

Figure 3.5: Radial Cross section of peripherally-adjacent stator cores of Z-TFM.

3.2 Conclusions

In this chapter, most of the basic topologies, namely single-sided TFM double-sided TFM, flux-concentrated transverse flux machines were presented. Though the single-sided TFM has lower torque density and lower power factor than other topologies, it is easier to construct and mechanically robust. Whereas other topologies have higher torque density and a better power factor but are difficult to construct and can be mechanically weak. The majority of the topologies present magnetic circuits that consist of a certain number of small-sized parts. These parts can advantageously be made of magnetic powder.

Chapter 4- Finite Element Analysis

In this chapter a brief introduction is given to the principle of finite element analysis (FEA) in electromagnetics and to the 3D FEA software Ansys Maxwell.

4.1 Introduction to Finite Element Analysis

Finite element analysis (FEA) is the core of every successful and innovative design of electromechanical design. It is based on a numerical calculation method called finite element method (FEM) which resolves various multi-physics problems in order to obtain the optimal approximate solutions which can improve the performance and the quality of any of electromechanical equipment.

The finite element method (FEM) is used to find approximate solution of partial differential equations (PDE) and integral equations. The solution approach is based either on eliminating the time derivatives completely (steady state problems), or rendering the PDE into an equivalent ordinary differential equation, which is then solved using standard techniques such as finite differences, etc.

In solving partial differential equations, the primary challenge is to create an equation which approximates the equation to be studied, but which is numerically stable, meaning that errors in the input data and intermediate calculations do not accumulate and destroy the meaning of the resulting output. There are many ways of doing this, with various advantages and disadvantages. The Finite Element Method is a good choice for solving partial differential equations over complex domains or when the desired precision varies over the entire domain.

In electromagnetics, the partial differential Equations to define a model is given by the complete set of Maxwell 's equations.

$$\vec{\nabla} \cdot \vec{B} = 0 \tag{4.1}$$

$$\vec{\nabla} \times \vec{H} = \vec{J} \tag{4.2}$$

Gauss' Law for electric field:

$$\Phi_E = \oiint_S \mathbf{E} \cdot d\mathbf{A} = \frac{q_{\text{enc}}}{\varepsilon_0} \tag{4.3}$$

or

$$\nabla \cdot \mathbf{E} = \frac{\rho}{\varepsilon_0} \tag{4.4}$$

Gauss' Law for magnetic field:

$$\Phi_B = \oiint_S \mathbf{B} \cdot d\mathbf{A} = 0 \tag{4.5}$$

or

$$\nabla \cdot \mathbf{B} = 0 \quad \text{(no magnetic monopole charges)} \tag{4.6}$$

Faraday's Law of Induction:

$$\oint_C \mathbf{E} \cdot d\mathbf{s} = -\frac{\partial}{\partial t} \int_S \mathbf{B} \cdot d\mathbf{A} \tag{4.7}$$

or

$$\nabla \times \mathbf{E} = -\frac{\partial \mathbf{B}}{\partial t} \tag{4.8}$$

Ampere's Law and Maxwell's Law of Induction:

$$\oint_C \mathbf{B} \cdot d\mathbf{s} = \mu_0 \varepsilon_0 \frac{d}{dt} \int_S \mathbf{E} \cdot d\mathbf{A} + \mu_0 i_{enc} \tag{4.9}$$

or

$$\nabla \times \mathbf{B} = \mu_0 \varepsilon_0 \frac{\partial \mathbf{E}}{\partial t} + \mu_0 \mathbf{j} \tag{4.10}$$

The main steps followed in a typical finite element analysis are shown in the figure below:

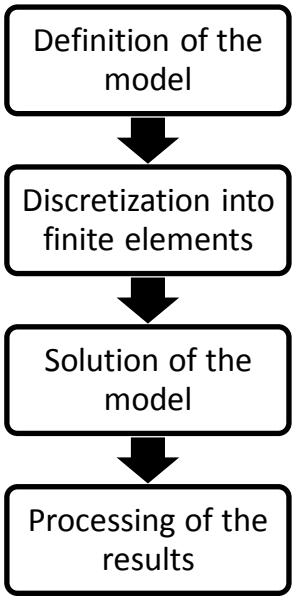

Figure 4.1: Flow Chart of the steps in finite element analysis

4.2 Introduction to Ansys Maxwell

Maxwell 3D is a high performance interactive software package that uses finite element analysis (FEA) to solve electric, magnetostatic eddy current and transient problems.

Maxwell solves the electromagnetic field problems by solving Maxwell's equations in a finite region of space with appropriate boundary conditions and when necessary with user-specified initial conditions in order to obtain a solution with guaranteed uniqueness.
The flow diagram used by Maxwell while solving the 3D field problems include Meshing, Computing Fields, Error Analysis and Solution.

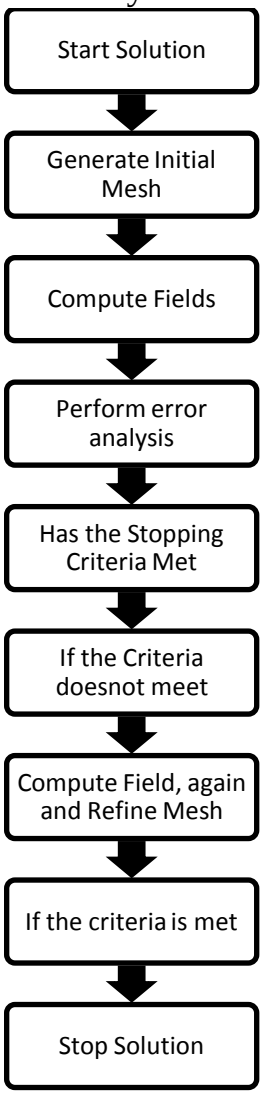

Figure 4.2: Flow Diagram Maxwell 3D uses to get the solution of 3D fields

4.3 Simulations in Maxwell 3D

4.3.1 Study of PM motor (2004 Prius IPM Motor)

It is an 8-pole permanent magnet motor with embedded magnets. The single layer windings are made of 3 phases. The stator has 48 slots. This motor is public, we therefore have the full set of parameters.

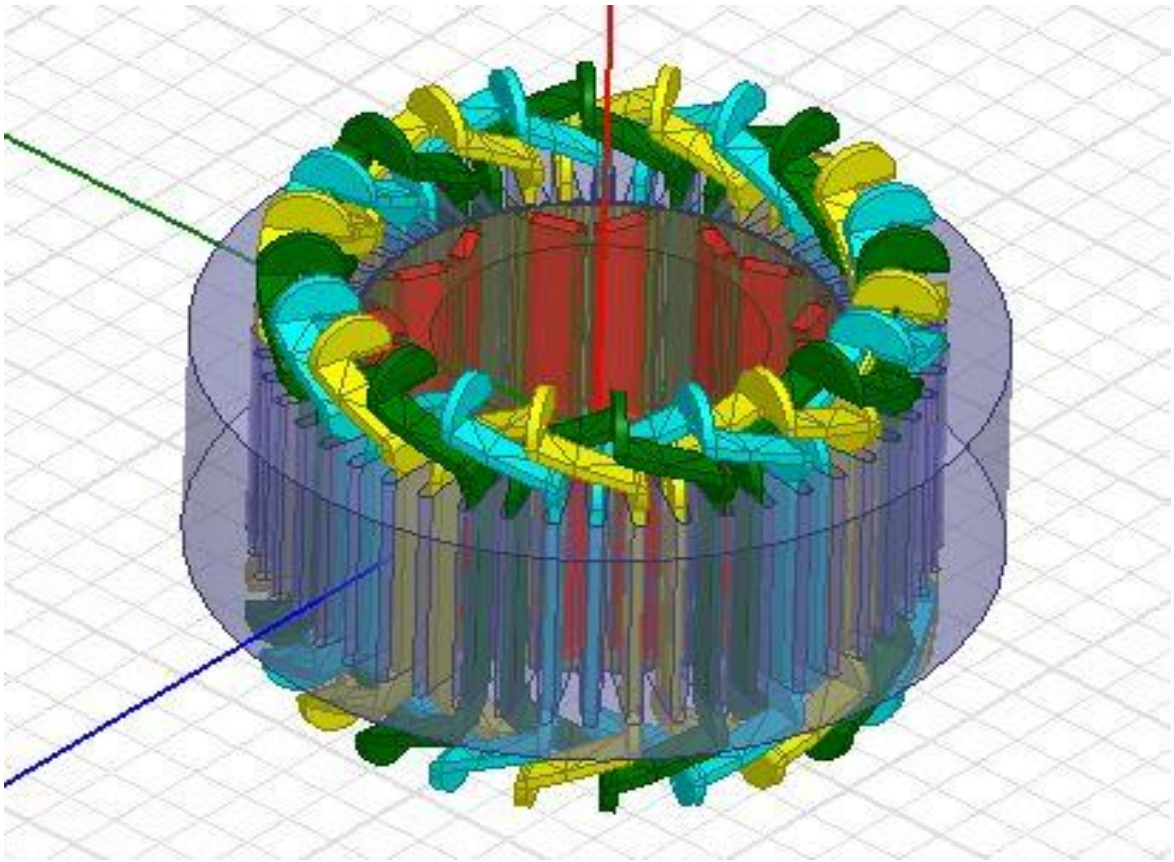

Figure 4.3: 3D Prius Motor drawn in Maxwell 3D

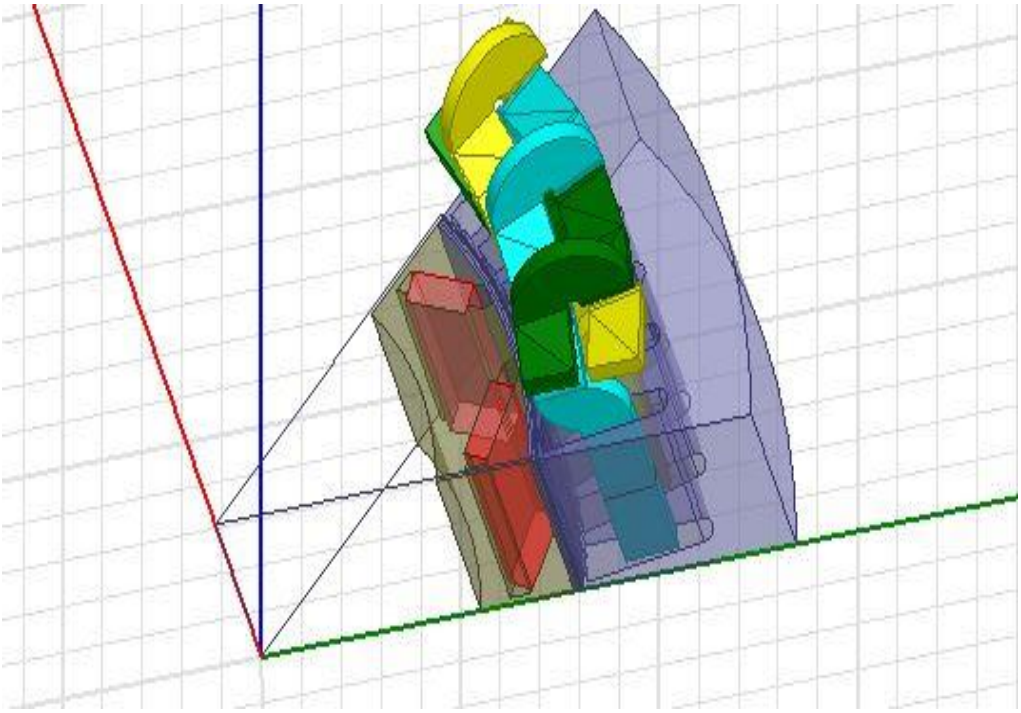

Figure 4.4: Reduced Portion Used For Simulation

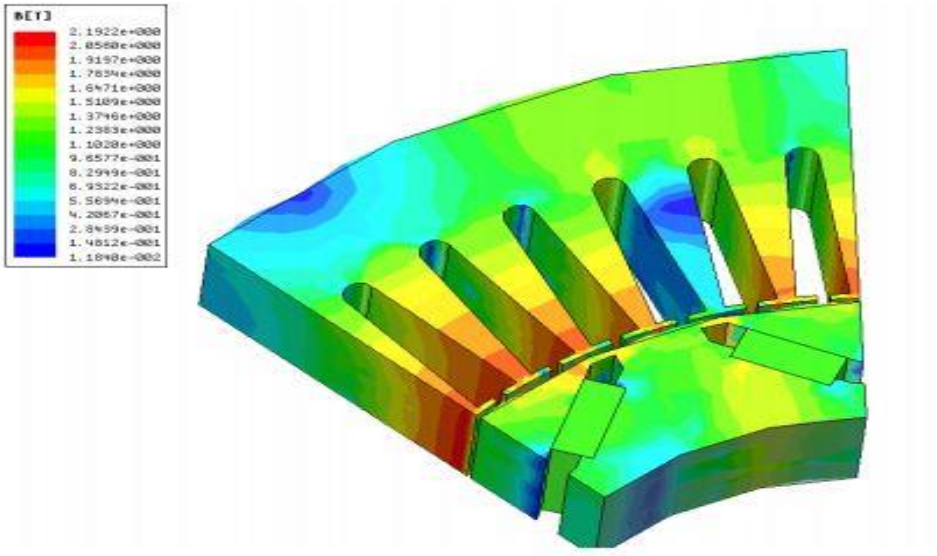

Figure 4.5: Magnetic Flux Density (Saturation)

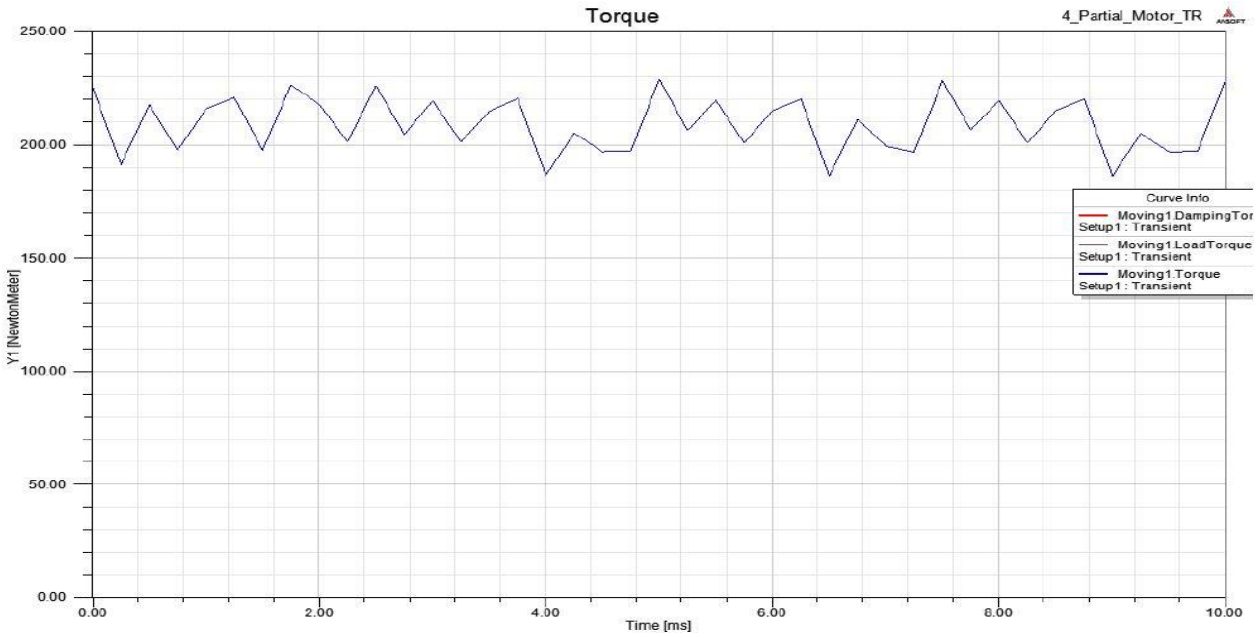

Figure 4.6: Torque Resulted from the Rotation of the Motor

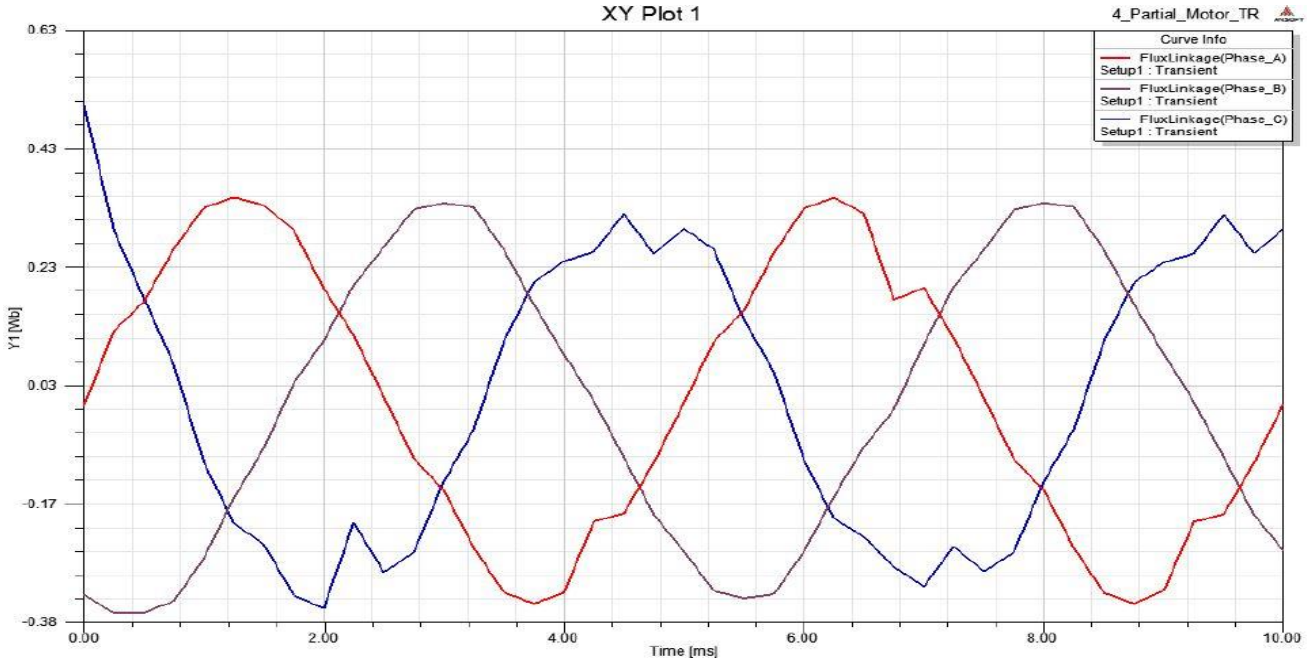

Figure 4.7: Flux Linkage of the Motor

4.3.2 Study of Transverse Flux Motor [1]

Transverse Flux Motor of the following dimensions obtained from the research in [1] is being implemented in Maxwell 3D software. The following figures will show the different portions and dimensions of the motor drawn in Maxwell 3D environment.

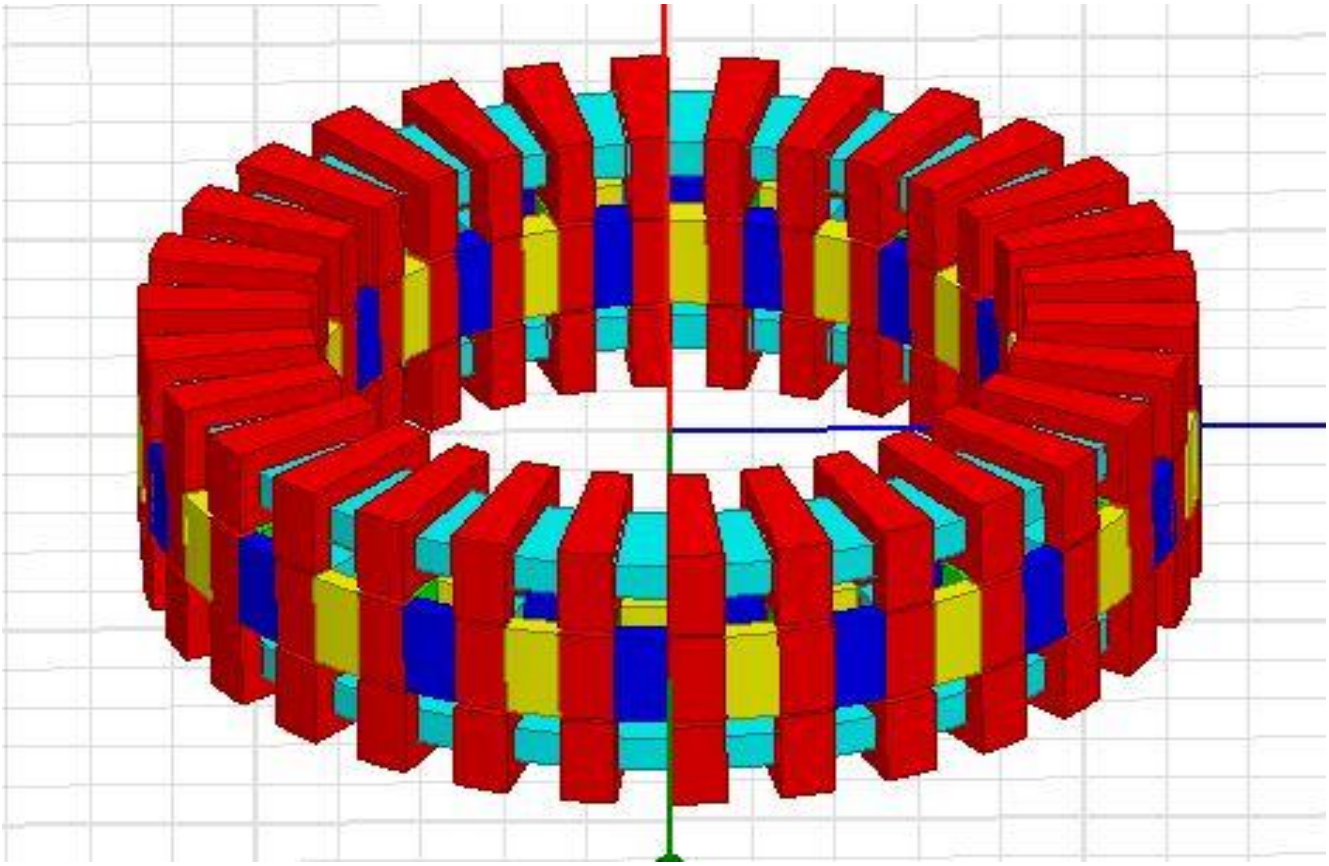

Figure 4.8: Full TFM

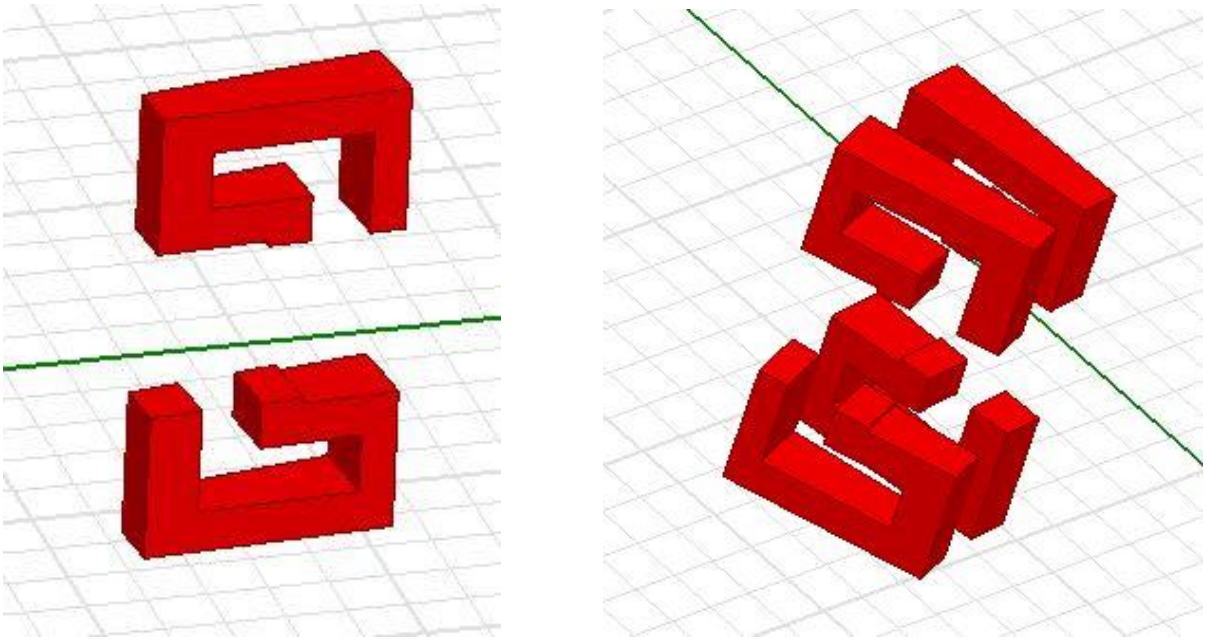

(a) (b)

Figure 4.9: Stator Parts of the TFM

Stator Geometry	
No. of Poles	30
No. of Phase	1
Slot Width	27mm
Slot Height	10mm
Slot Material	Steel

Table 4.1: Stator Geometry

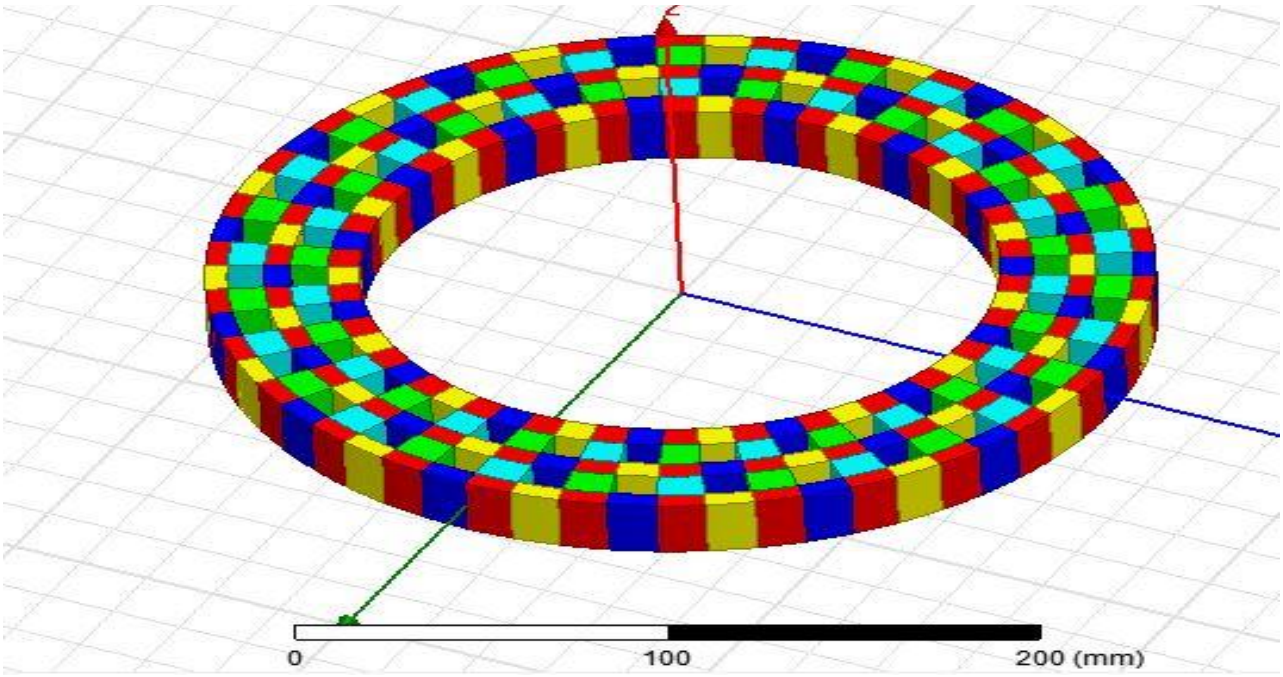

Figure 4.10: Circular Rotor with PMs sandwiched

Rotor Geometry	
Number of Poles	30
Inner Diameter	142mm
Outer Diameter	225mm
Thickness	26mm
Rotor Material	Steel

Table 4.2: Rotor Geometry

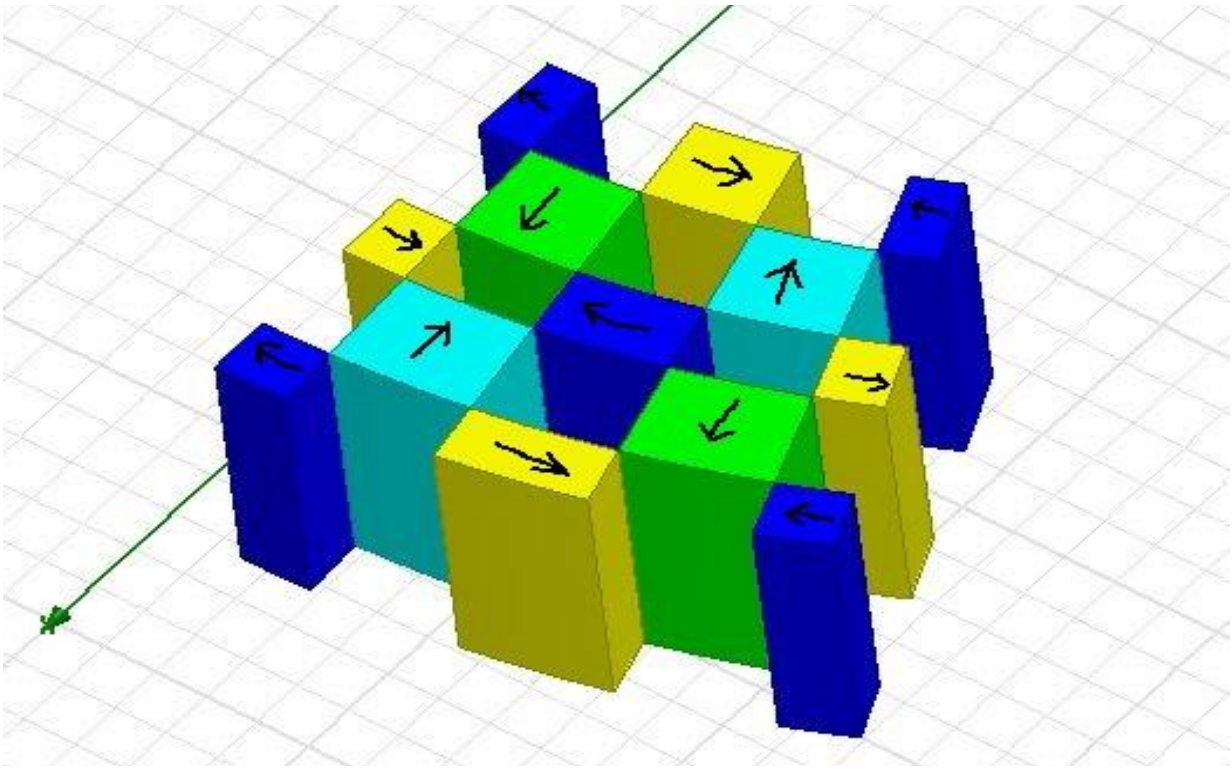

Figure 4.11: Magnet Geometry

Magnet Geometry	
Magnet Material	Ferrite
Relative Permeability	1.05
Remanence	0.4
Magnet Thickness	26mm

Table 4.3: Magnet Geometry

Design Specifications	
Rated Speed	400rpm
Current Density	5A/sq.mm
Air Gap	1mm
Outer Diameter	255mm
DC Bus Voltage	48V
Excitation Frequency	100Hz
Peak Current	105A
Air Gap Flux Density	1.2T
Axial Length	80mm

Table 4.4: Design Specifications

Chapter 5- Magnetic Equivalent Circuit

5.1 Magnetic Equivalent Circuit

Predicting the parameters and characteristics accurately for electromagnetic devices with complex geometry and high saturation can be quite involved and time requiring. Even special techniques are required to obtain relatively accurate results with advanced numerical methods like finite element method; in particular for design refinement or dynamic analysis programs in which repetitive computations are required. A method was therefore required which can combine both the speed of the conventional method and the flexibility of the FEA method. Magnetic Equivalent Circuit is a technique which is used to model electrical machines and can support both steady state and dynamic simulations. This method improves the numerical calculation and analysis for non-linear magnetic fields of electromagnetic devices. This numerical process is based on representation of magnetic material which is mainly comprised with a series of permeance elements. In this process, the flux from one tube never crosses the walls of the other tube. With the help of Gauss and Faraday's Laws, both Kirchoff's current law and voltage laws of basic electrical circuits are valid in these circuits. Electrical circuit matrix method is implemented here by sampling the flux into flux tubes. These are then named as permeance elements which gives produces a dual circuit with ampere turn sources.

The modelling of mmf in this design is made implementing the current carrying coil conductor and the permanent magnets. The polarity of the PMs gradually changes with the changes of rotor position due to the variation of rotor orientations of the magnets embedded in the rotor. For this reason, the calculation of flux has to be done very precisely and carefully for every rotation of the rotor. The electromagnetic characteristics of the TFM is repetitive and every pole has similar characteristics. In MEC approach, magnetic material characteristics and reluctance network based on machine geometry provides information about the magnetic saturation and leakage for FEA. As MEC technique requires less computational effort, it is much more advantageous to use in design optimization, control and modelling when juxtaposed to FEA technique.

The basic equations which determines each elements of the MEC design[23] is

$$F = \varphi R \tag{5.1}$$

Where, F, ϕ and R, are mmf, flux and reluctance respectively, and

$$R = \frac{L}{\mu_r \mu_o A_c} \tag{5.2}$$

Where μ_r, μ_o, A_c and L are the relative permeability, the permeability of free space, the cross-sectional area, and the length of each elements, respectively.

5.2 Modelling of MMF sources:

Each of the stator winding is modelled as an MMF source F_C,

$$F_c = NI \tag{5.3}$$

Where N is the number of turns and I is the phase current. Each permanent magnet machine is designed as an MMF source F_M in series with an internal reluctance R_M [24] where,

$$R_M = \frac{L_m}{\mu_{rm}\mu_o A_M} \tag{5.4}$$

$$F_M = \frac{L_m B_r}{\mu_{rm}\mu_o} \tag{5.5}$$

$$A_M = H_M L_A \tag{5.6}$$

μ_{rm} and B_r are the recoil permeability and remanence, respectively. A_M , L_M, L_A , and H_M are the cross-sectional area and thickness of the magnets in the direction of magnet field orientation, the axial length of the core and length of the magnets in the radial direction, respectively.

5.3 Flux Linkage:

The total flux linking which links the stator winding $\lambda(\theta)$ is obtained by

$$\varphi(\theta) = \frac{F_C + F_M}{R_T(\theta)} \tag{5.7}$$

$$\lambda(\theta) = N\varphi(\theta) \tag{5.8}$$

Where θ is the rotor position, R_T is the total machine reluctance including the rotor, stator, air gap and leakages. The flux entering the core of the TFM is a part of the flux present in the air gap. Armature leakage is the left part of the flux in the air gap [25]. Because of the presence of armature flux leakage all the flux that magnets produce do not enter the core and actually links the coil[26]. The detailed design for the air gap and leakage fluxes are discussed here.

5.4 EMF:

The flux through the core calculated earlier provides us with the EMF and so no load EMF is generated by the TFM. The EMF $e(\theta)$ is given by

$$e(\theta) = N\,\frac{\partial(\varphi)}{\partial(\theta)} \tag{5.9}$$

5.5 Torque:

Torque in an electrical machine can be defined as the rate of change of magnetic co-energy of its winding with respect to position [27]. Here MEC model has been integrated with virtual work method to envisage the torque in machines using air gap

flux information which is obtained during the change of rotor position. The virtual work method states that for a rotating machine, torque is given by

$$T = \frac{\partial W'(\theta,i)}{\partial \theta} \quad (5.10)$$

Where W' is the magnetic co-energy stored within the machine which is obtained by,

$$W'(\theta,i) = \int_{\{i=0\}}^{I} \lambda(\theta,i)di \quad (5.11)$$

Where λ is the flux linkage in the coils. It is more convenient in MEC method to keep the current constant instead of flux linkage. So the co-energy method is preferred here for the calculation of torque.

5.6 Air Gap Reluctance:

The flux tube in the air gap is the most vital component in MEC modelling. The energy is primarily stored in the air gap of the machine. It is generally difficult to establish a closed form of expression for the model as the rotor moves relatively with the stator and changes its position. So, the tube dimensions change as a function of rotor position. The tube reluctance, R_{airgap} which is a function of tube length,L cross-section area, A_c and magnetic permeability μ inside the tube [27] is given by,

$$R_{airgap} = \frac{L}{\mu_o A_c(\theta)} \quad (5.12)$$

$$dR = \frac{dx}{\mu A_c(\theta)} \quad (5.13)$$

$$R = \int \frac{dx}{\mu A_c(\theta)} \quad (5.14)$$

In general cases, the volume of the tube between the plates has a non-uniform or cross-sectional area. For such conditions, the volume of the tube is discretized to differential tube reluctance where dx is the differential tube length and $A_c(\theta)$ is the cross sectional area. The two components are then derived analytically. The total tube reluctance is calculated by the integration of differential reluctance over the entire tube length. The different types of reluctances that has been considered for the modelling of the machine are variable air gap reluctance, complete and partial pole overlap fringing reluctance, stator core fringing reluctance and winding leakage reluctance.

A)Variable Air Gap Reluctance:

There are usually two components for the variable air gap reluctance across the overlapping poles which depends upon the pole position. When the rotor changes position same stator pole can experience two different rotor poles with alternate flux paths. The sum of the two flux paths produced from the different overlapping rotor poles give the net flux path.

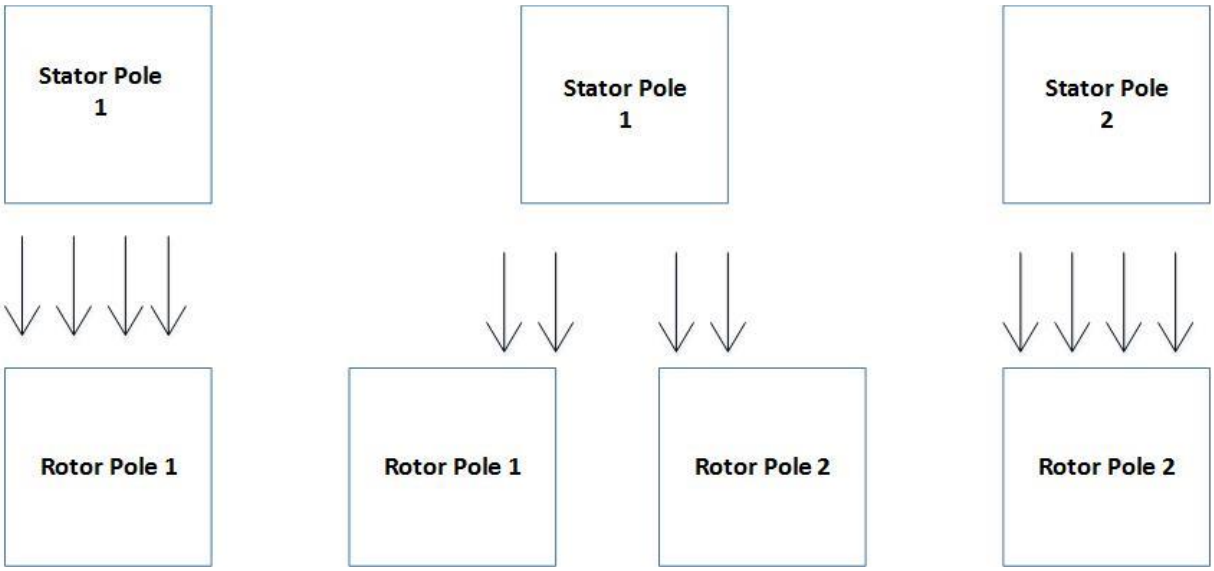

Figure 5.1: Variable Air Gap Reluctance

B) Partial Overlapping Fringing Reluctance:

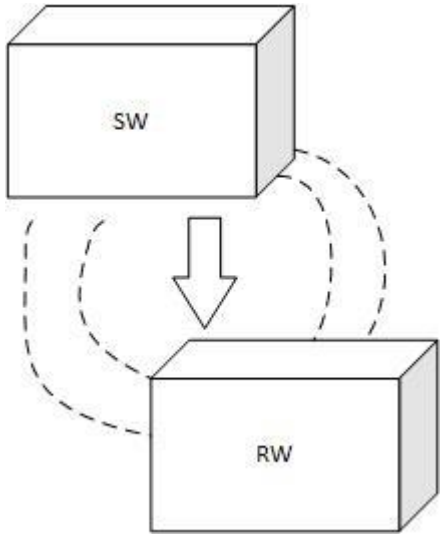

Figure: 5.2 Partial Overlapping Fringing Reluctance

The fringing field is portrayed as 90^0 wedge curve lines coming out of one pole and entering the side of the overlapping pole when there is partial overlap between the rotor and stator poles[26]. It is calculated by,

$$R_{poverlap1} = \frac{2\pi(shaft+lp1)}{8(\mu_o p)(shaft)(lp1)} \quad (5.15)$$

$$R_{poverlap2} = \frac{2\pi(shaft+lp1+magin+lp2)}{8(\mu_o p)(shaft+lp1+magin)(lp1)} \quad (5.16)$$

C) Complete Pole Overlapping Fringing Reluctance:

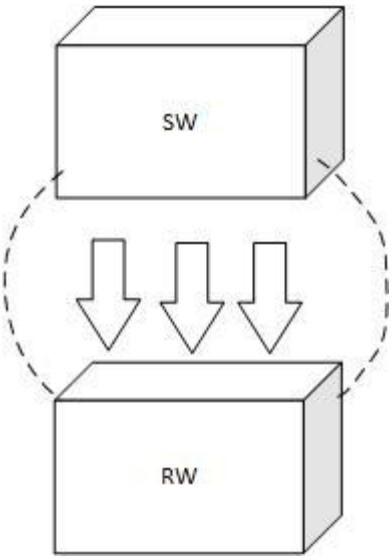

Figure 5.3: Complete Pole Overlapping Fringing Reluctance

At the time of complete overlapping between the rotor and stator poles, the flux tube is approximated by an 180 degree semicircle [26] as calculated by,

$$R_{overlap1} = \frac{2}{R_{overlap1}} \quad (5.17)$$

$$R_{overlap2} = \frac{2}{R_{overlap2}} \quad (5.18)$$

D) Stator Core Fringing Reluctance:

The possible flux paths through the air gap and the fringing paths around the air gap of the stator core is numbered serially from 1 to 4.

The semicircular line number 1 denotes the fringing path between the two stator pole faces. Assuming that the fringing between the planes form a volume of half annulus, the reluctance of fringing between planes is given by,

$$R_1 = \frac{\pi}{p\mu_o(rw2)\log((o.5lg+hry)/0.5\text{lg})} \quad (5.19)$$

The line 2 denotes the fringing between the two vertically-aligned parallel edges forming a volume of a quadrant of a spherical shell. The reluctance for fringing between these two parallel edges is given by

$$R_2 = \frac{4.34}{p\mu_o(rw2)} \quad (5.20)$$

Line 3 denotes the fringing between two aligned edges forming a volume of semicircular cylinder. The fringing reluctance between two aligned edges can be approximated by,

$$R_3 = \frac{4}{p\mu_o hry} \quad (5.21)$$

The final line 4 represents the fringing between the corners of the pole faces forming a volume of spherical quadrant. The reluctance is given by,

$$R_4 = \frac{6.5}{p\mu_o(0.5lg)} \tag{5.22}$$

E) Winding Leakage:

By using Biot-Savart law, the flux φ_w leaking the conductor can be calculated which is a function of the conductor radius R_c. The reluctance of the winding leakage R_w given by

$$d\varphi_w = dBA_{coil} \tag{5.23}$$

$$\varphi_w = \int_0^{\frac{\pi}{3}} d\phi = \frac{\mu_o NIR}{12} \tag{5.24}$$

$$R_w = \frac{\varphi_w}{NI} \tag{5.25}$$

Where A_{coil} is the cross-section area of the coil.

Chapter 6- Transverse Flux Motor

A new design has been established following the work of [1]. This new motor includes few modifications from the original work. The new TFM was designed in FLUX 3D software and the FEM analysis was performed on it. An analytical model was developed in Matlab Environment to match the properties of the motor obtained from the FEM analysis.

6.1. Geometry of TFM

6.1.1 Rotor Geometry:

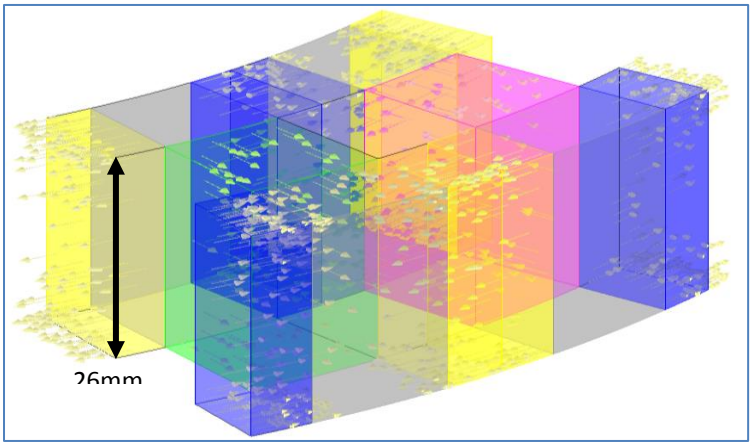

Figure 6.1 Rotor of New TFM

The rotor of the new TFM design consists of four permanent magnet parts. Each of the PM is sandwiched between the rotor poles. The rotor poles are made up of Steel and the permanent magnets are made up of Ferrite. The total number of rotor poles present in the TFM is 30. The height of the rotor is 26mm.

6.1.2 Stator Geometry: Each of the stator part is made up of steel like rotor parts. The height of the stator slot is 24m and the inner height is 17mm. The stator is of U-shape. The number of poles in the stator part is 15 but the stator is distributed alternatively in both the sides of the rotor.

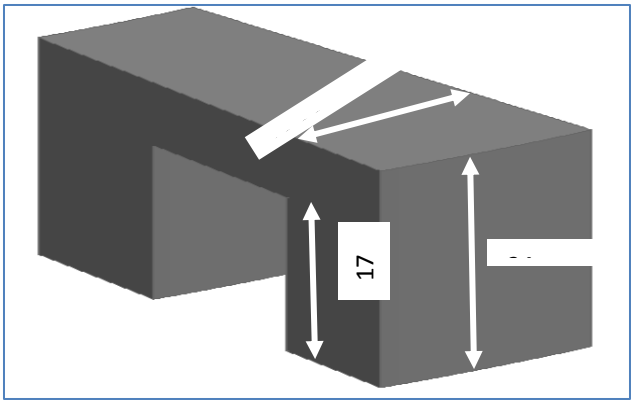

Figure 6.2: Stator of New TFM

6.1.3 Magnet Geometry:

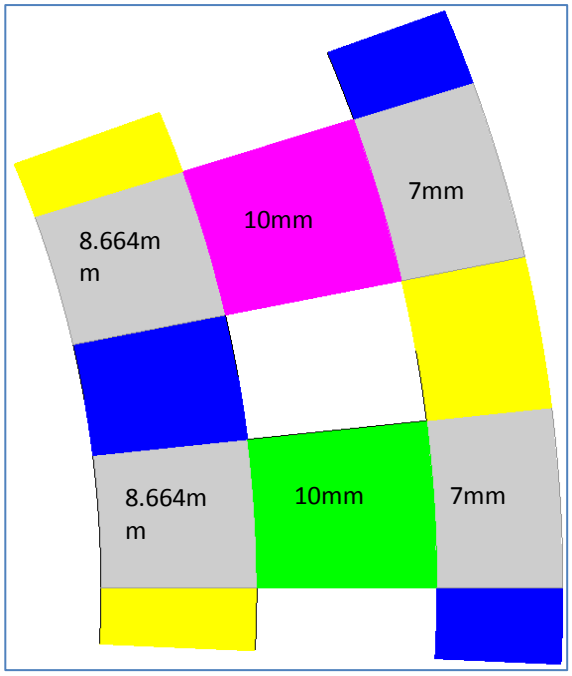

Figure 6.3 Magnet Geometry of New TFM

The magnet used in this TFM is permanent magnet and the material used for PM is ferrite. The relative permeability is 1.05 and the remanence of the magnet is 0.4. The

PMs sandwiched between two rotor arcs are of 10mm in length. The outer rotor arc contains PM of 7mm length and the inner arc rotor contains PM of 8.664mm.
The magnets are well directed in this TFM for completing the electrical equivalent circuit and have been provided with proper directions before conducting simulations. Each of the pink and green magnets are directed in opposite directions as well as the blue and the yellow PM parts. This alternate configuration in the direction allows the modular TFM to have once complete circuit.

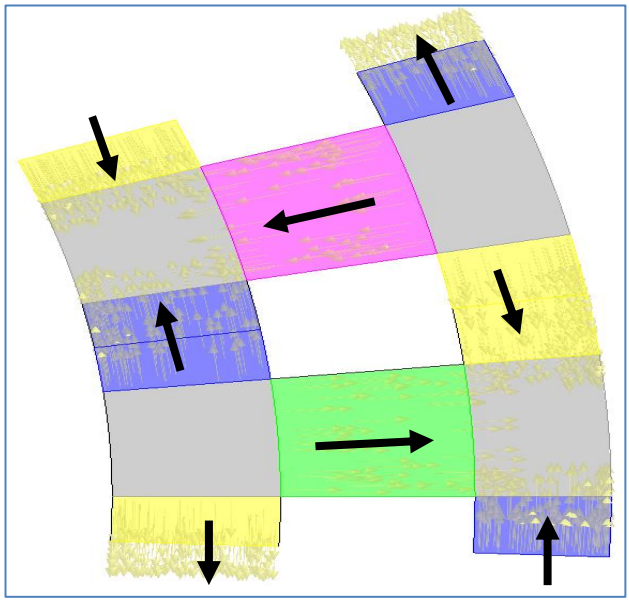

Figure 6.4: Permanent Magnet Directions

6.1.4 FULL TFM:

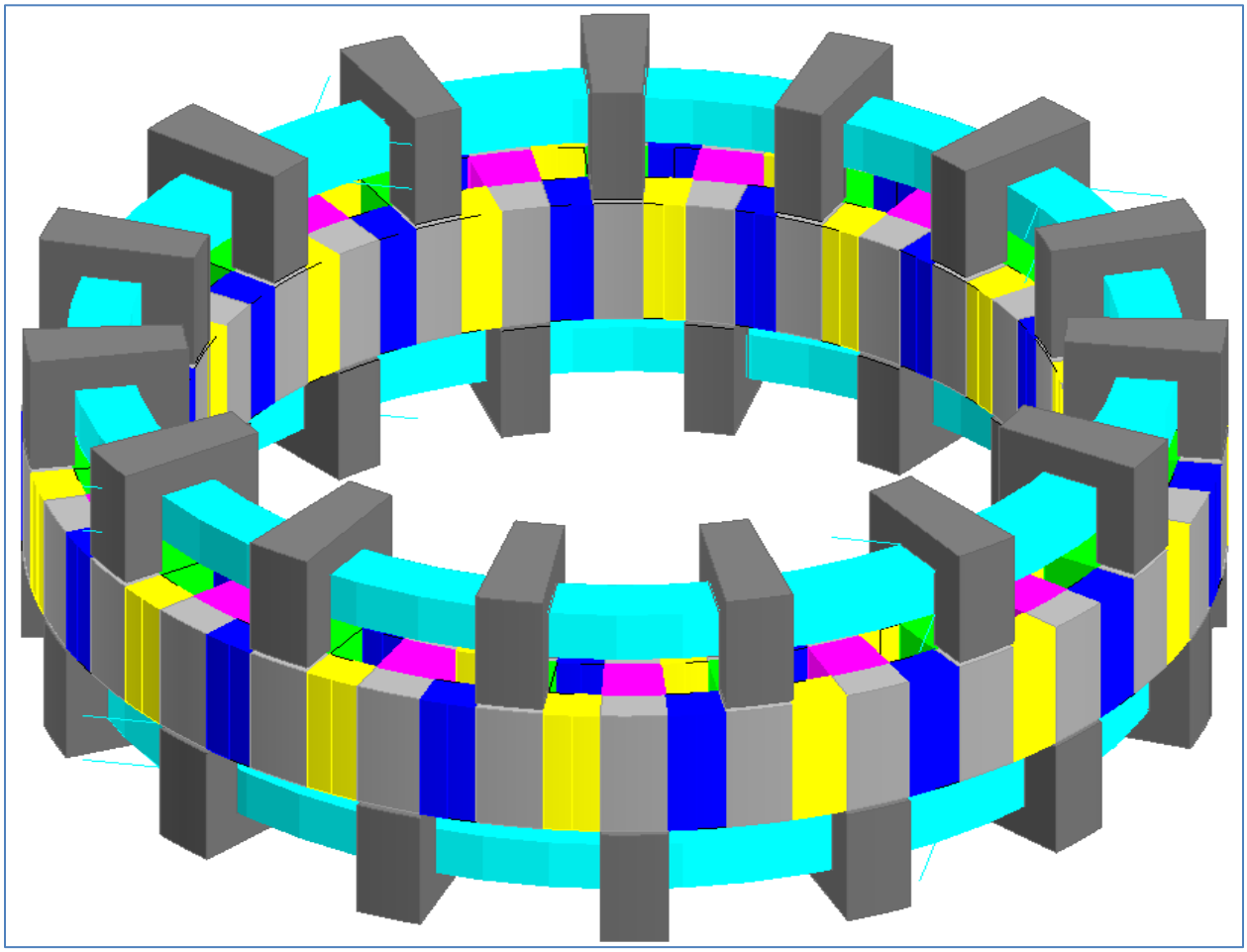

Figure 6.5: The full structure of TFM

6.2 Magnetic Equivalent Circuit of New TFM

The analytical circuit is modelled using the equations described in the previous chapter. The modelling does not include saturation calculation. The modelling includes no load modelling and loaded modelling. The new magnetic equivalent circuit of the new design is given below:

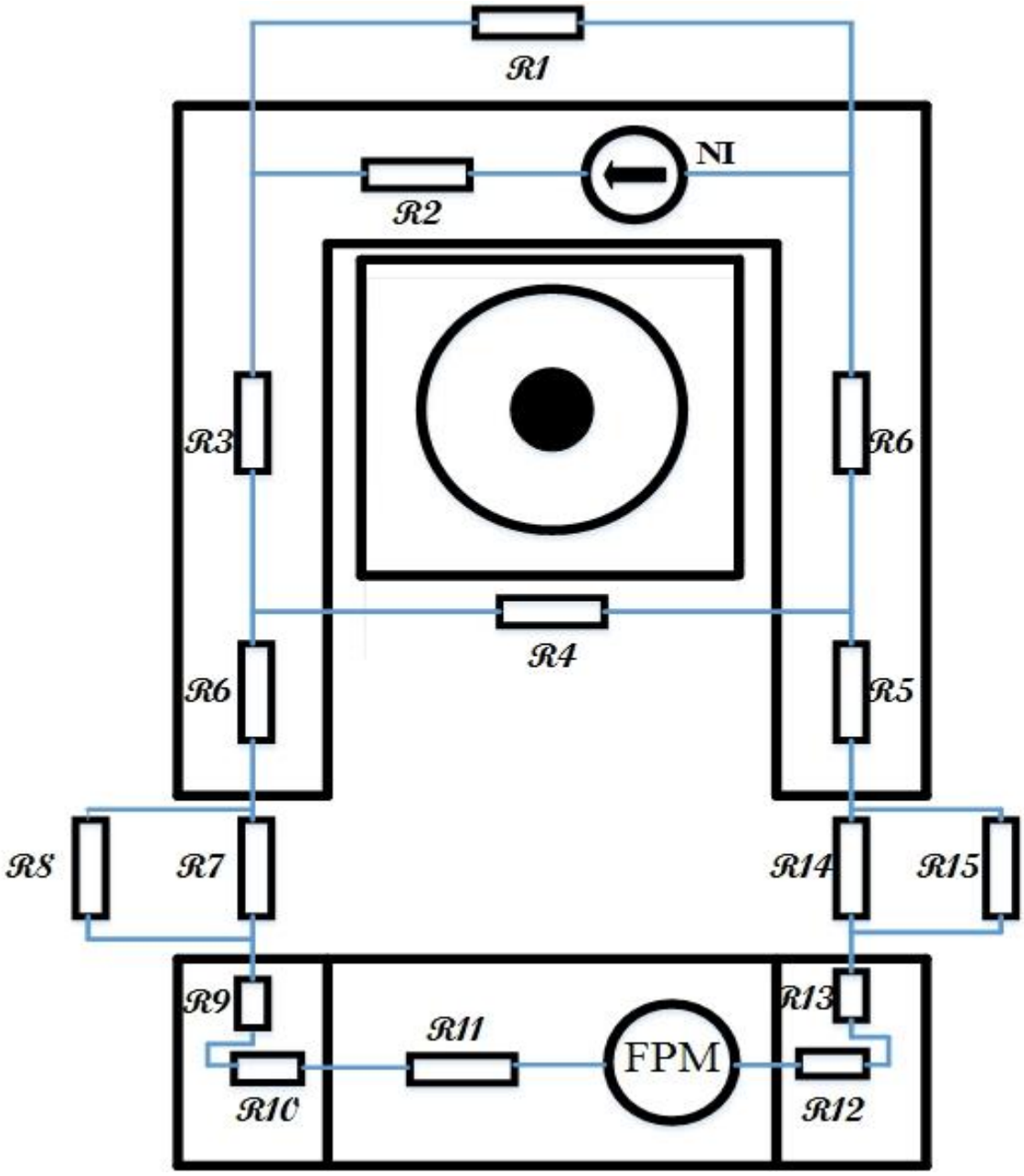

Figure 6.6: Magnetic Equivalent Circuit for one TFM pole

R1= Winding Leakage Reactance
R2,R3,R5,R6= Stator Iron Reluctance
R9,R10,R12,R13=Rotor Iron Reluctance
R11=Permanent Magnet Reluctance
R8,R15= Air Gap Fringing Reluctance
R7,R14= Air Gap Overlap Reluctance
NI= MMF from coil conductor
FPM= MMF from permanent magnet

6.3 Results

The MEC and 3D FEA model was based on dimensions stated before. The no-load flux linkage and EMF was determined for different rotor positions. Flux linkage and torque was also determined for different rotor positions while the coil conductor with different values of current for non-saturated conditions.

6.3.1 Flux Linkage, EMF and Torque at no load

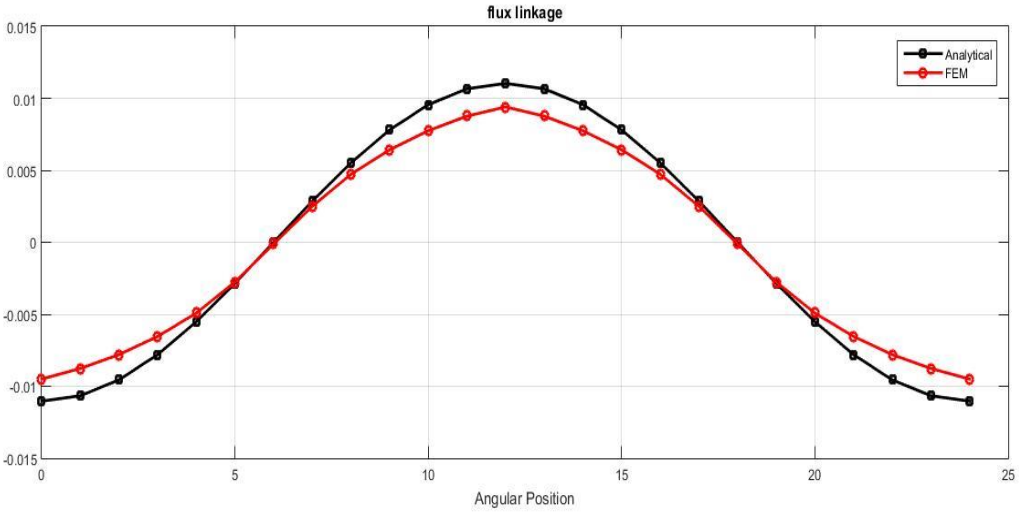

Figure 6.7: Flux Linkage comparison at 0A current or no load

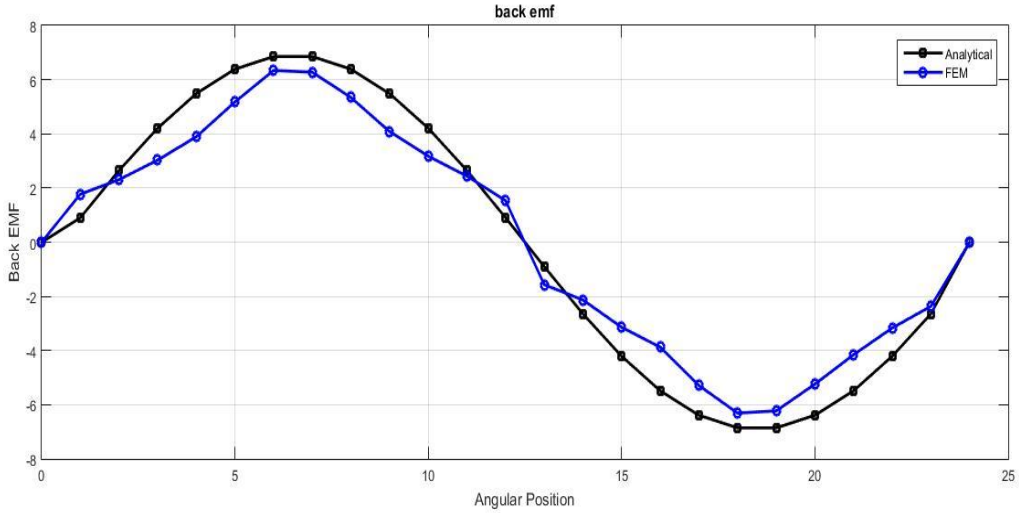

Figure 6.8: Back EMF comparison at 0A current or no load

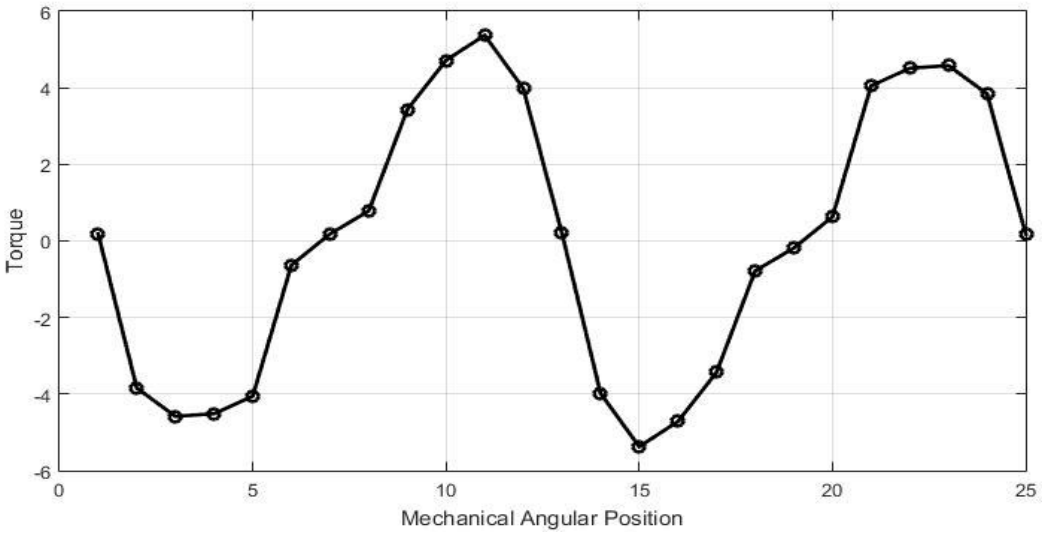

Figure 6.9: Torque at no-load condition

6.3.2 Flux Linkage, EMF and Torque at different Loads

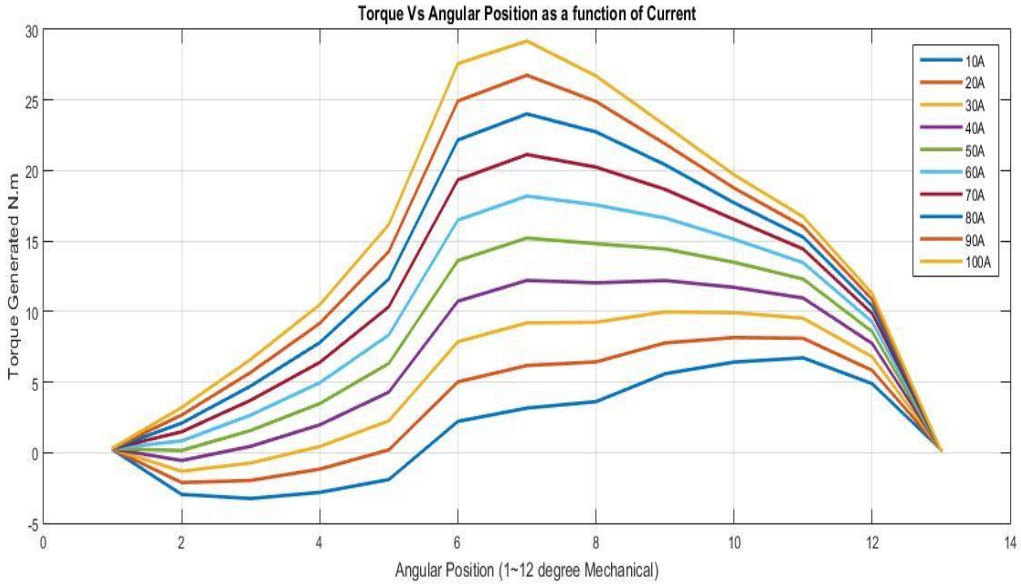

Figure 6.10: Torque generated at different loading conditions with respect to angular positions.

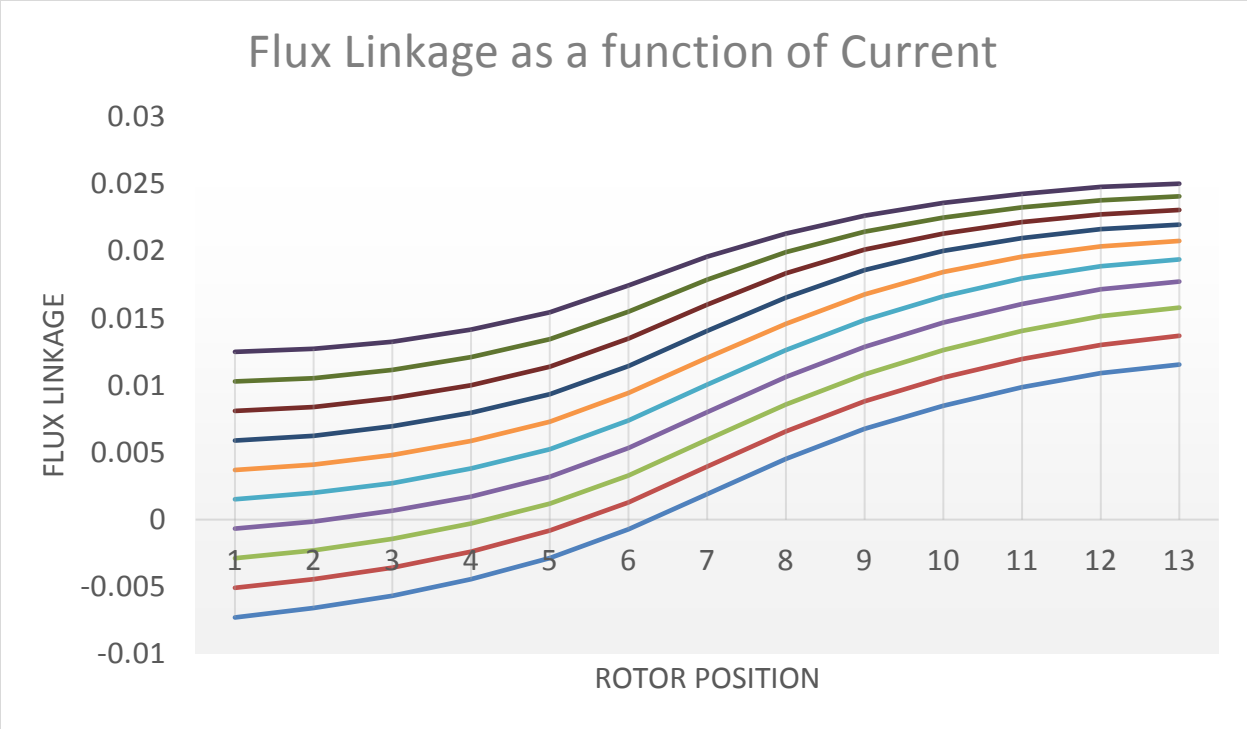

Figure 6.11: Flux Linkage at different loading conditions with respect to angular positions.

6.3.3 Torque at Full Load Condition

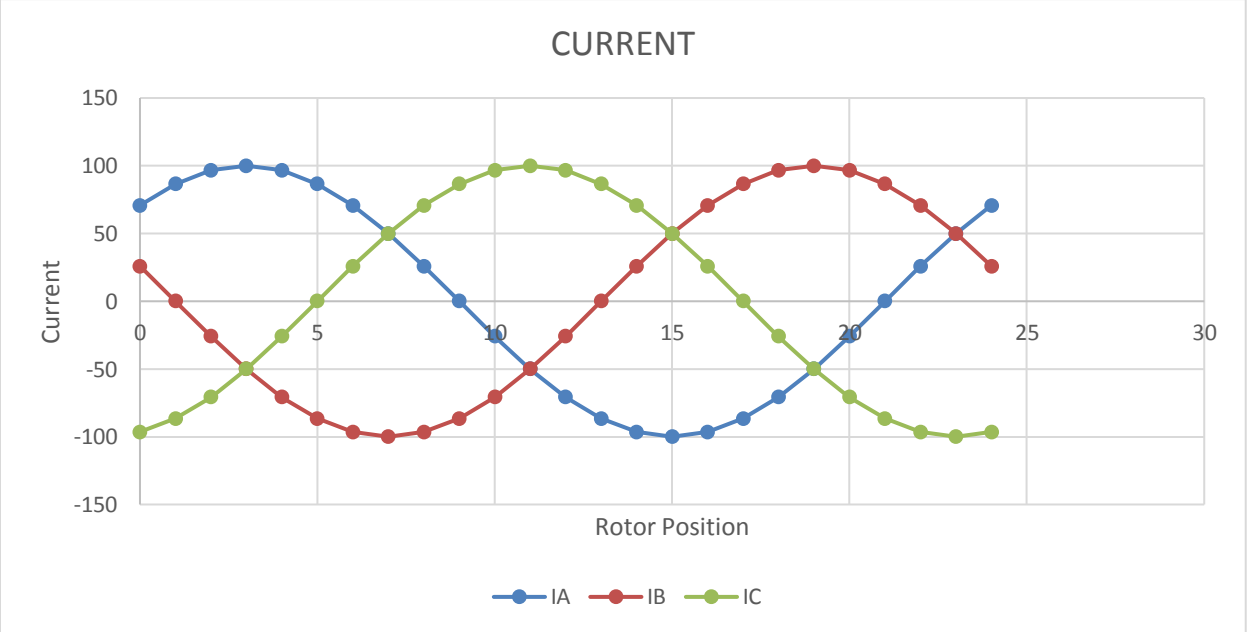

Figure 6.12: Full Load Current Input

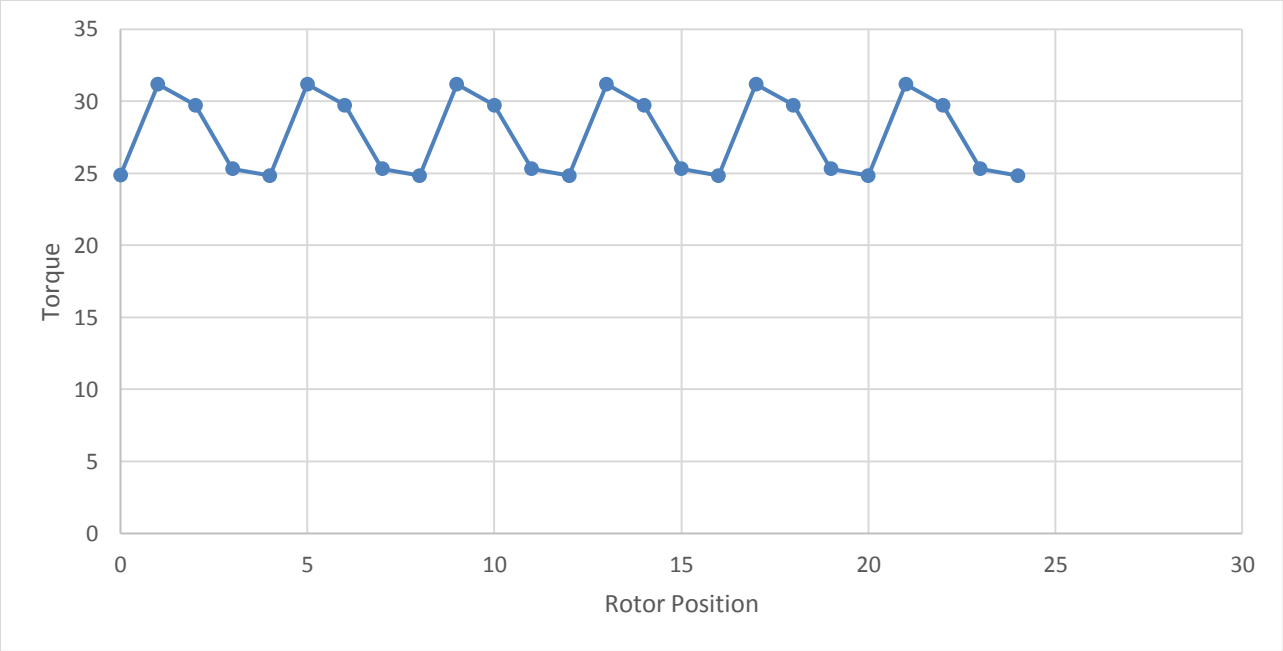

Figure 6.13: Full Load Torque.

6.3.4 Phase Cogging Torque

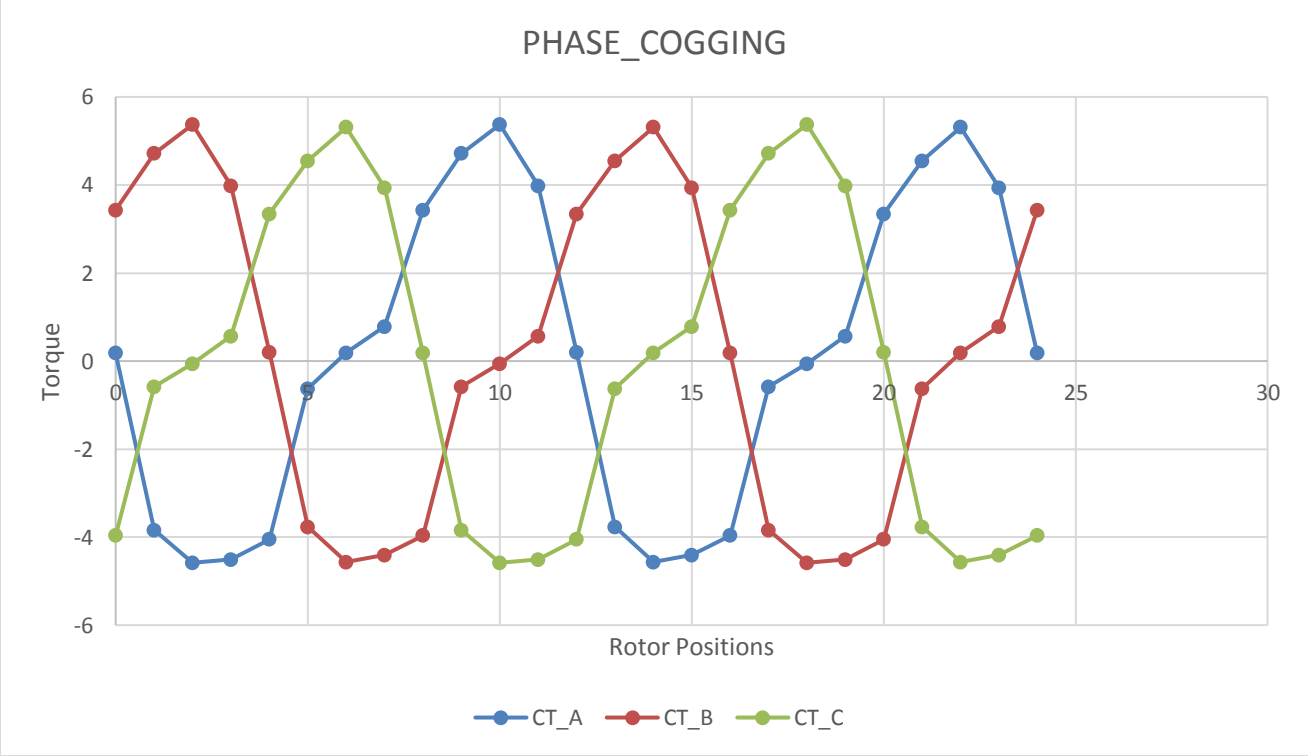

Figure 6.14: Phase Cogging Torque

Chapter 7- Conclusion

7.1 Future Works

In this work, it has been shown how analytically we can model a Transverse Flux Motor with minimum air-gap and less material and size. This work can be extended and developed to build stronger MEC model to apply saturation. Different optimization algorithms can be used to maximize the torque within a certain constraint of the geometries and dimensions. Algorithms like Genetic Algorithm, Particle Swarm Optimisation, MPSO etc have already proven to be successfully achieve results with less error. Nature inspired other algorithms can also be used in this Case. A prototype can be built to improve its performance. It could be interesting to study other topologies with an adapted analytical modelling.

7.2 Conclusion

A single phase, 1KW, 400 rpm Transverse Flux Motor has been analytically modelled here. The 3D model was developed using Flux 3D software. A dynamic MEC approach has allowed us to model the motor for its dimension and performance analysis with reduced computational resources. TFM requires magnets with high remanence in order to have high torque density. At the same time the torque density and the power factor are coupled inversely. The power factor of the transverse flux machine can be improved by sacrificing the torque density.

References

[1] Hasan, Iftekhar, Tausif Husain, Md Wasi Uddin, Yilmaz Sozer, Iqbal Husain, and Eduard Muljadi. "Analytical modeling of a novel transverse flux machine for direct drive wind turbine applications." In 2015 IEEE Energy Conversion Congress and Exposition (ECCE), pp. 2161-2168. IEEE, 2015.

[2] G. Kastinger, "Design of a novel transverse flux machine," in *proc. ICEM*, 2002.

[3] P. Anpalahan, "Design of transverse flux machines using analytical calculations& finite element Analysis," 2001.

[4] E. Laithwaite, *et al.*, "Linear motors with transverse flux," *Electrical Engineers, Proceedings of the Institution of*, vol. 118, pp. 1761-1767, 1971.

[5] H. Weh and H. May, "Achievable force densities for permanent magnet excited machines in new configurations," in *Proc. Int. Conf. Electrical Machines*, 1986, pp. 1107-1111.

[6] W. Arshad, *et al.*, "Analytical design and analysis procedure for a transverse flux machine," in *Electric Machines and Drives Conference, 2001. IEMDC 2001. IEEE International*, 2001, pp. 115-121.

[7] W. M. Arshad, *et al.*, "Use of transverse-flux machines in a free-piston generator," *IEEE transactions on industry applications*, vol. 40, pp. 1092-1100, 2004.

[8] U. Werner, *et al.*, "Stromregelung von Permanenterregten Transversalflussmotoren in Servo-Direktantriebsanwendungen," ed: DFMRS, 2006.

[9] I. Boldea and S. A. Nasar, *The induction machine handbook*: CRC press, 2010.

[10] L. Strete, *et al.*, "Optimal design of a rotating transverse flux motor (TFM) with permanent magnets in rotor," in *The XIX International Conference on Electrical Machines-ICEM 2010*, 2010.

[11] G. H. Pajooman, "Performance assessment and design optimisation of VRPM (transverse flux) machines by finite element computation," University of Southampton, 1997.

[12] Y. Rang, *et al.*, "Analytical design and modeling of a transverse flux permanent magnet machine," in *Power System Technology, 2002. Proceedings. PowerCon 2002. International Conference on*, 2002, pp. 2164-2167.

[13] G. Henneberger and M. Bork, "Development of a new transverse flux motor," in *New Topologies for Permanent Magnet Machines (Digest No: 1997/090), IEE Colloquium on*, 1997, pp. 1/1-1/6.

[14] S.-H. Han, *et al.*, "A magnetic circuit model for an IPM synchronous machine incorporating moving airgap and cross-coupled saturation effects," in *2007 IEEE International Electric Machines & Drives Conference*, 2007, pp. 21-26.

[15] M. Kremers, *et al.*, "Analytical flux linkage and EMF calculation of a transverse flux machine," in *Electrical Machines (ICEM), 2014 International Conference on*, 2014, pp. 2668-2673.

[16] P. Seibold and N. Parspour, "Analytical computation method of transverse flux permanent magnet excited machines via nodal analysis," in *Electrical Machines (ICEM), 2014 International Conference on*, 2014, pp. 410-415.

[17] E. Pădurariu, *et al.*, "A simple analytical model of a permanent magnet transverse flux motor with a particular disk rotor," in *Optimization of Electrical and Electronic Equipment (OPTIM), 2012 13th International Conference on*, 2012, pp. 641-646.

[18] M. Zafarani, *et al.*, "Analytical Model for a Transverse Flux Permanent Magnet Machine using Improved Magnetic Equivalent Circuit Approach," in *Systems Engineering (ICSEng), 2011 21st International Conference on*, 2011, pp. 96-99.
[19] Y. Kano, *et al.*, "A simple nonlinear magnetic analysis for axial-flux permanent-magnet machines," *IEEE Transactions on Industrial Electronics,* vol. 57, pp. 2124-2133, 2010.
[20] D.-K. Hong, *et al.*, "Optimum design of transverse flux linear motor for weight reduction and improvement thrust force using response surface methodology," *IEEE Transactions on Magnetics,* vol. 44, pp. 4317-4320, 2008.
[21] I. Hasan, *et al.*, "Analytical modeling of a novel transverse flux machine for direct drive wind turbine applications," in *2015 IEEE Energy Conversion Congress and Exposition (ECCE)*, 2015, pp. 2161-2168.
[22] V. Ostovic, "A simplified approach to magnetic equivalent-circuit modeling of induction machines," *IEEE Transactions on Industry Applications,* vol. 24, pp. 308-316, 1988.
[23] M. Moallem and G. Dawson, "An improved magnetic equivalent circuit method for predicting the characteristics of highly saturated electromagnetic devices," *IEEE Transactions on magnetics,* vol. 34, pp. 3632-3635, 1998.
[24] H. R. E. Devices and J. Wiley, "Sons," *Inc., New York,* p. 217, 1941.
[25] K. Lu, *et al.*, "Design considerations of permanent magnet transverse flux machines," *IEEE Transactions on magnetics,* vol. 47, pp. 2804-2807, 2011.
[26] M. Harris, *et al.*, "The problem of power factor in VRPM (transverse-flux) machines," in *Electrical Machines and Drives, 1997 Eighth International Conference on (Conf. Publ. No. 444)*, 1997, pp. 386-390.
[27] J. M. Kokernak and D. A. Torrey, "Magnetic circuit model for the mutually coupled switched-reluctance machine," *IEEE Transactions on magnetics,* vol. 36, pp. 500-507, 2000.
[28] J. Coulomb and G. Meunier, "Finite element implementation of virtual work principle for magnetic or electric force and torque computation," *IEEE Transactions on magnetics,* vol. 20, pp. 1894-1896, 1984.
[29] Wikipedia and Google Sources.